arXiv:2408.05201v3 [hep-th] 6 Nov 2024

Two-Loop Five-Point Two-Mass Planar Integrals and Double Lagrangian Insertions in a Wilson Loop

Samuel Abreu,[1,2] **Dmitry Chicherin,**[3] **Vasily Sotnikov,**[4] **Simone Zoia**[1]

[1] *Theoretical Physics Department, CERN, Geneva, Switzerland*

[2] *Higgs Centre for Theoretical Physics, School of Physics and Astronomy,*
The University of Edinburgh, Edinburgh EH9 3FD, Scotland, UK

[3] *LAPTh, Université Savoie Mont Blanc, CNRS, B.P. 110, F-74941 Annecy-le-Vieux, France*

[4] *Physik-Institut, University of Zurich, Winterthurerstrasse 190, 8057 Zurich, Switzerland*

E-mail: samuel.abreu@cern.ch, chicherin@lapth.cnrs.fr,
vasily.sotnikov@physik.uzh.ch, simone.zoia@cern.ch

ABSTRACT: We consider the complete set of planar two-loop five-point Feynman integrals with two off-shell external legs. These integrals are relevant, for instance, for the calculation of the second-order QCD corrections to the production of two heavy vector bosons in association with a jet or a photon at a hadron collider. We construct pure bases for these integrals and reconstruct their analytic differential equations in canonical form through numerical sampling over finite fields. The newly identified symbol alphabet, one of the most complex to date, provides valuable data for bootstrap methods. We then apply our results to initiate the study of double Lagrangian insertions in a four-cusp Wilson loop in planar maximally supersymmetric Yang-Mills theory, computing it through two loops. We observe that it is finite, conformally invariant in four dimensions, and of uniform transcendentality. Furthermore, we provide numerical evidence for its positivity within the amplituhedron region through two loops.

Contents

1 Introduction

Scattering amplitudes are essential components that bridge the formal aspects of quantum field theory with the observables that can be measured at particle colliders. Beyond the leading order in perturbation theory, these amplitudes are computed as sums of Feynman integrals which originate from the exchange of virtual particles. Indeed, understanding and being able to compute Feynman integrals is crucial in providing precise theoretical predictions for high-energy particle colliders such as the Large Hadron Collider (LHC). Besides their phenomenological importance, Feynman integrals are also interesting objects in their own right as their mathematical structure is very rich, with physical constraints being blended into complicated multi-valued functions. The calculation of Feynman integrals is thus central to the advancement of our understanding of quantum field theory, leading to both practical and theoretical advancements in particle physics.

While the functions which Feynman integrals evaluate to are generally not known (see ref. [1] for a recent review), many physically relevant Feynman integrals can be expressed as $\mathbb{Q}$-linear combinations of Chen's iterated integrals [2] over logarithmic differential one-forms, known as symbol letters. These so-called pure integrals [3] satisfy differential equations in canonical form [4] and possess several properties that make them particularly valuable for representing the transcendental functions involved in scattering amplitudes [5]. They provide compact and physically insightful representations of scattering amplitudes and are often suitable for efficient numerical evaluation. The intriguing relationship between symbols, leading singularities, and Landau singularities has gained considerable attention recently, with new methods having being developed to predict sets of symbol

letters [6–16], known as the alphabet. Additionally, certain constraints on the iterated integrals can sometimes be derived [17, 18], which can be leveraged into bootstrap approaches to systematically construct and verify the structure of scattering amplitudes. These provide a powerful method to explore and understand the underlying physics without relying solely on explicit calculations.

It is a priori not known if a set of Feynman integrals contributing to a given scattering processes can be represented in this form. While several methods have been devised to facilitate finding such representations [19–28], in the case of multi-scale Feynman integrals this still remains a very challenging task. At two loops, among the most complex cases considered are all integrals for five-point one-mass scattering [29–31], some integrals for six-point massless scattering [32], as well as selected integral topologies relevant for $t\bar{t}j$ and $t\bar{t}H$ in hadron collisions [33–35] (although in the latter cases not all integrals were found to be pure). The first five-point integral topology with two external masses has been considered in ref. [14]. These calculations all follow a similar pattern: one finds a good basis for the space of Feynman integrals under consideration, and then obtains the corresponding differential equations. In some cases the solutions in terms of iterated integrals can be efficiently evaluated numerically [31, 36, 37].

In this work we consider the complete set of planar two-loop five-point integrals with two off-shell external legs. These integrals are relevant, for instance, for the yet unknown second-order corrections in the strong-coupling constant for the production of two heavy vector bosons production in association with a jet or a photon, or for the third-order QCD corrections to the production of two heavy vector bosons. We find that it is possible to construct sets of so-called master integrals whose differential equations are in canonical form [4], that is where the dependence on the dimensional regulator factorises and only logarithmic one-forms with algebraic arguments appear. We employ finite-field techniques [38–40] to reconstruct the differential equations. The logarithmic forms, or symbol letters, mostly but not completely match the results predicted by the method of ref. [14]. Even if incomplete, the partial knowledge of the symbol alphabet greatly simplifies the task of reconstructing the analytic differential equation. We find that the complexity of the alphabet increases substantially compared to the case where a single external leg is off-shell [29].

The Feynman integrals that we calculate in this work are also interesting for studies of more formal aspects of QFT. We are motivated by the renowned duality between the vacuum expectation values of the null polygonal Wilson loops and scattering amplitudes in maximally super-symmetric Yang-Mills theory (MSYM) [41–43]. This duality suggests the definition of a class of finite gauge-invariant multi-scale observables in MSYM which are closely related to the scattering amplitudes and their integrands [44]. We consider the correlations functions of the null Wilson loop and several Lagrangians, normalised by the vacuum expectation value of the null Wilson loop. This ratio of correlation functions is finite and is expected to possess a number of intriguing properties, as we discuss in this paper. We refer to it as Lagrangian insertions in the null Wilson loop.

The case of a single Lagrangian insertion in the four-cusp Wilson loop has been extensively studied in the literature. It is calculated at strong coupling [45] and at weak coupling up to three-loop order [46–48]. The single Lagrangian insertion in multi-cusp Wilson loop has been studied in [49], where hidden symmetries and dualities with pure Yang-Mills amplitudes have been revealed. The single Lagrangian insertion in the five-cusp Wilson loop has been calculated in the two-loop approximation in [50]. A recent inspiring development in the perturbative study of the single Lagrangian insertion in the four-cusp Wilson loop originated from its geometric description. The four-dimensional loop integrands of scattering amplitudes are completely specified by the amplituhedron [51]. However, the implications of the amplituhedron construction are less transparent for integrated amplitudes, which require infrared regularisation. Unlike amplitudes, the Lagrangian insertion in the Wilson loop is well-defined in four space-time dimensions, and the geometric constructions for the four-dimensional loop integrands can be promoted to the integrated loop corrections. A decomposition of the loop corrections into negative geometries has been studied

in refs. [52, 53], and certain geometries have been solved and resummed to all loop orders. The negative geometry decomposition has been also extended to the ABJM theory [54–56].

Given the numerous beautiful properties observed for the single Lagrangian insertion, it is natural to wonder if these also hold for double Lagrangian insertions. In this work we initiate the study of double Lagrangian insertions. We consider the double Lagrangian insertion in the four-cusp null Wilson loop, which is the simplest null polygonal contour, and calculate it for the first time through two loops. As compared to the single Lagrangian insertion, the kinematic space of the double Lagrangian insertion is multidimensional already for the four-cusp contour considered in this paper. The perturbative two-loop calculation we perform here supports the expectation that the double Lagrangian insertion is finite, conformally invariant in four dimensions, and has uniform transcendentality. The fact that these properties emerge from our calculation give a strong check of the correctness of the integrals we compute in this paper.

Another remarkable geometric observation focuses on the positivity of the integrated loop corrections of the single Lagrangian insertion. More precisely, relying on the available perturbative data, it was observed in refs. [49, 52] that the loop corrections of the single Lagrangian insertion have uniform sign in a certain subregion of the Euclidean kinematic region which is predicted by the amplituhedron construction. Recently, ref. [57] provided evidence that the positivity of the loop corrections could be extended to a much stronger statement of complete monotonicity, which restricts the sign of the derivatives of all orders in kinematic variables. In this work we provide numerical evidence that the integrated loop corrections of the double Lagrangian insertion have uniform sign inside the amplituhedron region, at least up to two loops.

The paper is organised as follows. In section 2 we discuss our notation and conventions for the integrals considered in this paper. In section 3, we discuss the pure bases of master integrals and the corresponding analytic differential equations, including the determination of the alphabet relevant for the description at two loops of planar scattering processes involving five particles, out of which two are off shell. We also provide sample numerical evaluations and discuss the checks we performed. In section 4 we present the calculation of the double Lagrangian insertion in a (quadrilateral) Wilson loop at the two-loop order. We summarise our results and discuss some possible next steps in section 5. We conclude with two appendices. In appendix A we list our master integrals for all the five-point sectors of the two-loop families. In appendix B we define a number of kinematic regions relevant in this work. Our ancillary files are available at [58].

2 Kinematics and Definitions

2.1 Kinematics

We compute all two-loop planar integrals required to describe scattering processes involving five external legs, out of which three are massless and two are massive. All internal propagators are massless. The momenta of the massless external legs are denoted p_1, p_2 and p_3, and the momenta of the two massive legs are denoted p_4 and p_5. We take the momenta to be outgoing, and they satisfy the momentum-conservation relation

$$p_1 + p_2 + p_3 + p_4 + p_5 = 0 \,. \tag{2.1}$$

With these kinematics, there are seven independent Mandelstam variables, which we choose to be

$$X := \left\{ s_{12}, s_{23}, s_{34}, s_{45}, s_{15}, s_4, s_5 \right\} , \tag{2.2}$$

with $s_{ij} := (p_i + p_j)^2$ and $s_i := p_i^2$. We work in dimensional regularisation, with $d = 4 - 2\epsilon$ spacetime dimensions and four-dimensional external momenta.

The kinematics of these processes are also described by Gram determinants. We define them as

$$\mathrm{Gram}\big(\{a_1,\ldots,a_m\},\{b_1,\ldots,b_m\}\big) \coloneqq \det\big(2\,a_i\cdot b_j\big)\big|_{i,j=1,\ldots,m}\,,$$
$$\mathrm{Gram}(a_1,\ldots,a_m) \coloneqq \mathrm{Gram}\big(\{a_1,\ldots,a_m\},\{a_1,\ldots,a_m\}\big)\,. \tag{2.3}$$

In particular, we will need

$$\Delta_3(p_i,p_j) \coloneqq \mathrm{Gram}\big(p_i,p_j\big) = -\lambda(s_i,s_j,s_{i,j})\,, \tag{2.4}$$
$$\Delta_5 \coloneqq \mathrm{Gram}\big(p_1,p_2,p_3,p_4\big)\,, \tag{2.5}$$

where $\lambda(x,y,z)$ is the Källén function,

$$\lambda(x,y,z) \coloneqq x^2 + y^2 + z^2 - 2xy - 2yz - 2zx\,. \tag{2.6}$$

The Gram determinant Δ_5 is related to the five-particle pseudo-scalar invariant via

$$\Delta_5 = \mathrm{tr}(\slashed{p}_1\slashed{p}_2\slashed{p}_3\slashed{p}_4\gamma_5)^2\,. \tag{2.7}$$

We also use Gram determinants to express the (-2ϵ)-dimensional components of the loop momenta, conventionally denoted μ_{ij}, in terms of scalar products of external and loop momenta:

$$\mu_{ij} \coloneqq k_i^{[-2\epsilon]}\cdot k_j^{[-2\epsilon]}\,,$$
$$= \frac{\mathrm{Gram}\big(\{k_i,p_1,p_2,p_3,p_4\},\{k_j,p_1,p_2,p_3,p_4\}\big)}{2\,\Delta_5}\,, \tag{2.8}$$

where $k_i =: k_i^{[4]} + k_i^{[-2\epsilon]}$, with $k_i^{[-2\epsilon]}\cdot p_j = 0 = k_i^{[-2\epsilon]}\cdot k_j^{[4]}$. These objects play an important role in the construction of compact pure integral bases (see section 3).

2.2 Integral Families

The set of integrals we will compute can be organised into two one-loop families and six two-loop families, distinguished by the relative position of the two massive legs. They are depicted in figs. 1 and 2, together with our convention for the routing of the loop momenta and the naming of each family. Each diagram in figs. 1 and 2 is associated with a set of master integrals. For instance, to the diagram of fig. 1a we associate a vector space corresponding to integrals of the form

$$I_{\mathrm{Pa}}(\vec{\nu}) = \int \frac{\mathrm{d}^{4-2\epsilon}k\,e^{\epsilon\gamma_E}}{\mathrm{i}\,\pi^{2-\epsilon}}\,\frac{1}{\rho_1^{\nu_1}\rho_2^{\nu_2}\rho_3^{\nu_3}\rho_4^{\nu_4}\rho_5^{\nu_5}}$$
$$= \int \mathcal{D}^{4-2\epsilon}k\,\frac{1}{(k^2)^{\nu_1}}\frac{1}{[(k+p_1)^2]^{\nu_2}}\frac{1}{[(k+p_1+p_2)^2]^{\nu_3}}\frac{1}{[(k-p_4-p_5)^2]^{\nu_4}}\frac{1}{[(k-p_5)^2]^{\nu_5}} \tag{2.9}$$

for integer ν_i. We omit Feynman's prescription for the propagators. Each element in this vector space corresponds to a set of exponents $\vec{\nu}$, and in this paper we compute a basis of this space. In eq. (2.9), we introduced the integration measure in dimensional regularisation

$$\mathcal{D}^{4-2\epsilon}k \coloneqq \frac{\mathrm{d}^{4-2\epsilon}k\,e^{\epsilon\gamma_E}}{\mathrm{i}\,\pi^{2-\epsilon}}\,, \tag{2.10}$$

which also defines the normalisation of our integrals. The inverse propagators ρ_i can be read off the diagram in fig. 1a, where we included a (red) index for each propagator. The corresponding expression for the second one-loop family, denoted $I_{\mathrm{Pb}}(\vec{\nu})$, can be easily obtained from fig. 1b.

At two loops, the diagrams in fig. 2 are not sufficient to fully specify our conventions, as we must also define the so-called irreducible scalar products (ISPs). To each diagram in fig. 2 we associate a vector space corresponding to integrals of the form

$$I_F(\vec{\nu}) = \int \mathcal{D}^{4-2\epsilon}k_1\,\mathcal{D}^{4-2\epsilon}k_2\,\frac{\rho_9^{-\nu_9}\rho_{10}^{-\nu_{10}}\rho_{11}^{-\nu_{11}}}{\rho_1^{\nu_1}\rho_2^{\nu_2}\rho_3^{\nu_3}\rho_4^{\nu_4}\rho_5^{\nu_5}\rho_6^{\nu_6}\rho_7^{\nu_7}\rho_8^{\nu_8}}\,, \tag{2.11}$$
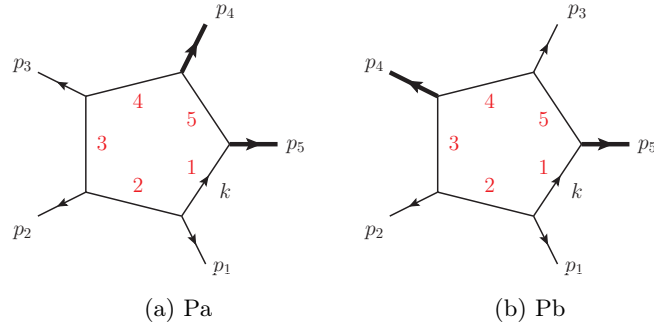
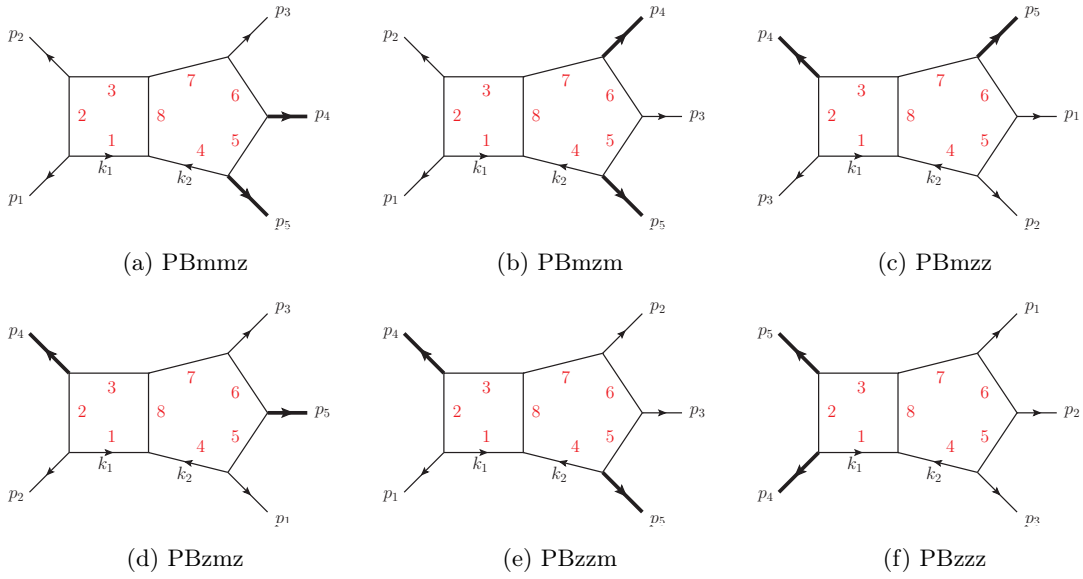Figure 1: Independent set of one-loop "pentagon" topologies.

Figure 2: Independent set of two-loop "pentagon-box" topologies.

with $F \in \{\text{PBmmz, PBmzm, PBmzz, PBzmz, PBzzm, PBzzz}\}$ and for integer ν_i such that $\nu_i \leq 0$ for $i = 9, 10, 11$. The complete set of definitions for all the families considered in this paper can be found in our ancillary files [58].

The dimension $\dim(F)$ of the vector space associated with each family F in figs. 1 and 2 corresponds to the number of master integrals we must compute for each of them. We collected these numbers in table 1. We determined them by generating systems of integration-by-parts (IBP) relations [59, 60] with LiteRed [61, 62] and NeatIBP [63], and solving them with the Laporta algorithm [64] within the finite-field framework FiniteFlow [40, 65].

We close the discussion of integral families with two comments. First, we do not consider here two-loop families that are products of one-loop integrals, as they can be trivially obtained from the integrals computed in this paper. Second, all planar integral topologies for instance "triangle-hexagon", are reducible to the integrals from pentagon-box topologies computed here.

Family	$\dim(F)$	$\dim(\mathcal{A}_F)$		Family	$\dim(F)$	$\dim(\mathcal{A}_F)$
Pa	16	43		PBmzz	105	80
Pb	15	39		PBzmz	104	96
PBmmz	94	85		PBzzm	104	82
PBmzm	87	52		PBzzz	127	104

Table 1: The number of master integrals $\dim(F)$, and the dimension of the alphabet $\dim(\mathcal{A}_F)$ of each family F.

3 Pure Bases and Canonical Differential Equations

A pure basis and canonical differential equations for PBzzz were already obtained in ref. [14]. In this section, we discuss the construction of pure bases [3] of master integrals (MIs) for all families. Let $\vec{I}_F$ be the list of all MIs for the family F. We say that $\vec{I}_F$ is pure if it satisfies a system of differential equations (DEs) in the canonical form [4]

$$\mathrm{d}\vec{I}_F(X, \epsilon) = \epsilon\, \mathrm{d}A_F(X) \cdot \vec{I}_F(X, \epsilon)\,, \tag{3.1}$$

where the connection matrix $A_F(X)$ is given by a $\mathbb{Q}$-linear combination of logarithms,

$$A_F(X) = \sum_i a_i^{(F)} \log\left(W_i(X)\right)\,. \tag{3.2}$$

Here, d is the total differential with respect to the kinematic invariants in X (see eq. (2.2)),

$$\mathrm{d} = \sum_{x \in X} \mathrm{d}x\, \frac{\partial}{\partial x}\,, \tag{3.3}$$

$a_i^{(F)}$ is a matrix of rational numbers, and the $W_i(X)$'s are algebraic functions of X called letters. The ensemble of all letters, called the alphabet and denoted $\mathcal{A}_F$ below, encodes the singularity structure of the MIs. We devote section 3.2 to the identification of the letters and the expression of the connection matrices in terms of them, and focus here on the problem of constructing a basis $\vec{I}_F$ such that the dimensional regulator ϵ factorises as in eq. (3.1).

Given a list of candidate MIs $\vec{I}_F(X, \epsilon)$, we differentiate it using LiteIBP [40, 65], and rewrite the derivatives in terms of $\vec{I}_F(X, \epsilon)$ by solving IBP relations. We generate the required IBP relations using LiteRed [61, 62] and NeatIBP [63]. The latter provides optimised systems of IBP relations by solving syzygy equations [66], allowing for a faster and less memory-consuming solution. We solve the IBPs via the Laporta algorithm [64] within the finite-field framework FiniteFlow [40, 65]. This allows us to side-step the intermediate expression swell which plagues multi-variable computations by replacing the symbolic manipulations with numerical evaluations over finite fields [38, 39]. In other words, all rational coefficients are evaluated numerically for random integer values of all variables X and ϵ modulo some (large) prime number.

The complete factorisation of ϵ requires the introduction of several square roots. A number of approaches have been proposed to include them in the finite-field framework, e.g. by sampling over phase-space points where the arguments of the roots are perfect squares in the finite field (see e.g. [29]). These approaches are however inconvenient when there are many distinct square roots. Following ref. [40], we prefer to reconstruct the DEs for what we call "pre-canonical" bases $\vec{I}_F'$, i.e., bases whose MIs are pure up to overall normalisation by square-root factors. In other words, their DEs take the form

$$\frac{\partial \vec{I}_F'(X, \epsilon)}{\partial x} = \left[A_{F,x}^{(0)}(X) + \epsilon\, A_{F,x}^{(1)}(X)\right] \cdot \vec{I}_F'(X, \epsilon)\,, \tag{3.4}$$

for all $x \in X$, where $A_{F,x}^{(0)}(X)$ and $A_{F,x}^{(1)}(X)$ are matrices of rational functions, and $A_{F,x}^{(0)}(X)$ is diagonal, with non-zero entries only in correspondence with those MIs which require a square-root normalisation. The finite-field sampling of the matrices $A_{F,x}^{(k)}(X)$ can then proceed via the standard algorithms. We perform the functional reconstruction by following the strategy described in e.g. refs. [67, 68], based on fitting linear relations among the rational coefficients and matching factors against an ansatz over univariate phase-space slices. We also set $s_{12} = 1$ and restore its dependence via dimensional analysis. With these techniques and the optimised IBP relations generated by NEATIBP, the functional reconstruction of the DEs for the pre-canonical bases is fairly simple.

Finally, we achieve the factorisation of ϵ with a basis transformation

$$\vec{I}_F(X, \epsilon) = N_F(X) \cdot \vec{I}_F'(X, \epsilon), \tag{3.5}$$

where the transformation matrix is diagonal and satisfies the DEs

$$\frac{\partial N_F(X)}{\partial x} + N_F(X) \cdot A_{F,x}^{(0)}(X) = 0 \tag{3.6}$$

for all $x \in X$. We obtain the analytic expression of $N_F(X)$ by solving these DEs. Alternatively, one may determine it by computing the leading singularities [3], but we find this to be unnecessary in this case as the DEs in eq. (3.6) are fairly simple to solve. We recall that, by construction, $N_F(X)$ contains only the square-root normalisations. In other words, $N_F(X)^2$ is a rational function. The resulting DEs for $\vec{I}_F(X, \epsilon)$ take the ϵ-factorised form in eq. (3.1), where the connection matrix $A_F(X)$ satisfies

$$\frac{\partial A_F(X)}{\partial x} = N_F(X) \cdot A_{F,x}^{(1)}(X) \cdot N_F^{-1}(X), \tag{3.7}$$

for all $x \in X$.

In section 3.1 we discuss how we constructed the pre-canonical integral bases. In section 3.2 we describe the alphabet, how we obtained it, and how we express the connection matrices $A_F(X)$ in terms of logarithms of letters, as in eq. (3.2). Section 3.3 is devoted to the initial conditions necessary to solve the DEs, to the solution of the DEs using DIFFEXP, and to the validation of our results. Finally, in section 3.4 we discuss how the canonical DEs and the initial conditions allow us to straightforwardly obtain the associated symbols [69] and write the integrals in terms of Chen iterated integrals [2].

3.1 Construction of the Pure Bases

We organise the construction of the integral bases sector by sector, starting from the lowest, i.e., the one with the fewest propagators. We first analyse each sector on its maximal cut. This amounts to focusing on the diagonal block of the connection matrices which couples the MIs of the chosen sector. We refer to this part of the DEs as the homogeneous part. Once the diagonal block of a given sector is in pre-canonical form, we extend the analysis to include all its sub-sectors. A basis which is canonical on the maximal cut may still require sub-sector corrections to be pure. If the entry ij in the in-homogeneous part of the connection matrix is not ϵ-factorised, we modify the definition of the ith MI by a term proportional to the jth MI, and fix the coefficient by imposing the factorisation of ϵ in the entry under consideration. This approach requires the analytic expression of the relevant entries of the DEs. As mentioned above, obtaining it is not a bottleneck in this case, provided that the integral basis is already (pre-)canonical on the maximal cut. This in fact ensures that the analytic expression of the connection matrices is substantially simpler than with an arbitrary basis. Once a sector is fixed, we proceed to all its super-sectors, until we reach the top sector.

We construct candidate pure bases for the sectors with fewer than five external legs by mapping pure integrals taken from the literature onto our definitions. In particular, we make use of the results of ref. [28] for the planar two-loop four-point integrals with three external massive legs, and of ref. [29] for the MIs that overlap with those appearing in planar two-loop five-point integrals with one external massive leg.

For the genuinely five-point sectors, we build upon the knowledge about two-loop five-point integral families with other external mass configurations available in the literature. More precisely, we draw from refs. [29, 34, 35]. We take their choices of MIs, naïvely change the kinematics to ours, and make manual adjustments to achieve the factorisation of ϵ. This process is particularly simple for integrals written in terms of the loop-momentum scalar products μ_{ij} defined in eq. (2.8) since, unlike the same expressions after expansion in terms of scalar integrals, they have trivial generalisations to different kinematic configurations. We emphasise that, in order to analyse the dependence on ϵ of the pure candidates constructed in this way, it suffices to reconstruct the ϵ dependence of the connection matrices, that is, it suffices to work on a univariate slice where all kinematic variables X are set to random values, which is computationally inexpensive.

The top sectors of all families but PBzzz have 3 MIs each. Following the pattern known in the literature [29, 34, 35], we find that the following numerators give rise to pure integrals:

$$
\begin{aligned}
\mathcal{N}_F^{(1)} &= \epsilon^4 \sqrt{\Delta_5}\, (p_{F,i} + p_{F,j})^2\, \mu_{12}\,, \\
\mathcal{N}_F^{(2)} &= \epsilon^4 \sqrt{\Delta_5}\, (p_{F,i} + p_{F,j})^2\, \mu_{22}\,,
\end{aligned}
\tag{3.8}
$$

where $p_{F,i}$ and $p_{F,j}$ are the external momenta attached to the box sub-graph. For the third MI in the top sector, the literature suggests to start from a numerator proportional to $(k_2 - q_F)^2$, where q_F is the external momentum on the bottom left of the graphs in fig. 2. In addition to an overall normalisation factor, we find that a simple sub-sector correction is required for some of the families. Explicitly, we find

$$
\begin{aligned}
\mathcal{N}_{\text{PBmmz}}^{(3)} &= \epsilon^4\, s_{12}(s_4 s_{12} - s_{34} s_{45})\,(k_2 - p_1)^2\,, \\
\mathcal{N}_{\text{PBmzm}}^{(3)} &= \epsilon^4\, s_{12}(s_4 s_5 - s_4 s_{34} - s_5 s_{34} - s_{12} s_{34} + s_{34}^2 + s_{34} s_{45})\,(k_2 - p_1)^2\,, \\
\mathcal{N}_{\text{PBmzz}}^{(3)} &= \epsilon^4\, s_{12} s_{15} \left[s_{34}\,(k_2 - p_3)^2 - s_4\, k_2^2 \right]\,, \\
\mathcal{N}_{\text{PBzmz}}^{(3)} &= \epsilon^4\, (s_4 s_{15} - s_4 s_5 + s_{12} s_{15} + s_5 s_{23} + s_5 s_{34} - s_{15} s_{34} - s_{15} s_{45}) \left[s_{24}\,(k_2 - p_2)^2 - s_4\, k_2^2 \right]\,, \\
\mathcal{N}_{\text{PBzzm}}^{(3)} &= \epsilon^4\, s_{23}(s_4 + s_5 + s_{12} - s_{34} - s_{45}) \left[s_{14}\,(k_2 - p_1)^2 - s_4\, k_2^2 \right]\,.
\end{aligned}
\tag{3.9}
$$

Unlike the cases above, the top sector of the family PBzzz has 4 MIs. It was already studied in ref. [14], but we provide here a new representation of the pure basis in terms of μ-insertions for a subset of the MIs. Indeed, three of them can be chosen as above:

$$
\begin{aligned}
\mathcal{N}_{\text{PBzzz}}^{(1)} &= \epsilon^4 \sqrt{\Delta_5}\, s_{45}\, \mu_{12}\,, \\
\mathcal{N}_{\text{PBzzz}}^{(2)} &= \epsilon^4 \sqrt{\Delta_5}\, s_{45}\, \mu_{22}\,, \\
\mathcal{N}_{\text{PBzzz}}^{(3)} &= \epsilon^4\, s_{45} \left[s_{12} s_{23}\,(k_2 - p_4)^2 - s_{12} s_{15}\, k_2^2 - s_{23} s_{34}\,(k_2 - p_4 - p_5)^2 \right]\,.
\end{aligned}
\tag{3.10}
$$

For the fourth MI we could not find a simple representation, and we adopted the definition from ref. [14]. The expression is lengthy and we thus omit it here. We limit ourselves to highlighting that its normalisation involves two square roots (of Δ_5 and of $\lambda(s_4, s_5, s_{45})$), and that a simple numerator which yields ϵ-factorised DEs on the maximal cut is

$$
\mathcal{N}_{\text{PBzzz}}^{(4)'} = \epsilon^4\, s_{45} \sqrt{\Delta_5} \sqrt{\lambda(s_4, s_5, s_{45})}\, \frac{2\,(k_2 - p_4)^2\, \mu_{12} + (s_{45} - s_4 - s_5)(\mu_{12} + \mu_{22})}{\lambda(s_4, s_5, s_{45})} + (\text{sub-sectors})\,.
\tag{3.11}
$$

We present our pure bases for all the other five-point sectors in appendix A. The complete bases can be found in the ancillary files [58].

3.2 Analytic Differential Equations and Alphabet

Having determined pure bases for each family, we now turn to obtaining analytic DEs in the form of eqs. (3.1) and (3.2). The main missing ingredient are the set of letters of the alphabet corresponding to each family, i.e., the logarithms in eq. (3.2). Despite having analytic DEs, casting them in the form of eqs. (3.1) and (3.2) still requires to integrate the entries of the DE matrices to identify the letters. In practice, we find it more convenient to follow the approach of ref. [30, 70], where the letters are not obtained directly from the DEs, and the analytic differential equations are obtained by numerically fitting the matrices $a_i^{(F)}$ in eq. (3.2) once the alphabet is known.

In order to determine the letters for each of the families in fig. 2 we rely on recent developments in constructing symbol alphabets [9–14, 16], in particular on the implementation of the ideas of ref. [14] in the `Mathematica` library `Baikovletter`. In this section, we discuss which letters could be determined using ref. [14], and which letters we had to construct ourselves.[1]

The first question we can ask about the alphabets $\mathcal{A}_F$ associated with each of the integral families we consider in this paper is their dimension, that is the number of linearly independent (combinations of) dlogs that appear in the associated differential equations. Answering this question does not require knowledge of the analytic form of the dlogs, and we collect the alphabet dimensions in table 1.

Once the dimension of the alphabet is known, we have a target for the number of letters we must construct for each family. Based on previous experience [30], we distinguish several types of letters. First, we have even letters that are polynomials in the Mandelstam variables. Second, we have odd letters which change their sign together with the sign of the square roots that were introduced to construct the pure basis. Odd letters can depend on either a single square root $\sqrt{\Lambda}$ or two square roots $\sqrt{\Lambda_1}$ and $\sqrt{\Lambda_2}$. In the first case we assume they take the form

$$\frac{p(X) + q(X)\sqrt{\Lambda}}{p(X) - q(X)\sqrt{\Lambda}}, \tag{3.12}$$

and in the second case they take the form

$$\frac{p(X) + q(X)\sqrt{\Lambda_1}\sqrt{\Lambda_2}}{p(X) - q(X)\sqrt{\Lambda_1}\sqrt{\Lambda_2}}, \tag{3.13}$$

where $p(X)$ and $q(X)$ are polynomials in X. Odd letters have the property that they are singular at places where the even letters vanish [30, 71, 72]. Given that the square roots are known, this observation can be used to constrain the polynomials $p(X)$ and $q(X)$ and thus construct candidate odd letters. Finally, we note that in the alphabet corresponding to five-point one-mass kinematics at two loops we found that we could always set $q(X) = 1$, but this is not possible for the two-mass case.

We used the `Mathematica` package `Baikovletter` [14] to identify most of the alphabet for each of the families in fig. 2 (the alphabet of the one-loop families in fig. 1 is a subset of the two-loop one). For PBmmz, PBmzz and PBzzz, the letters identified in this way exactly span the space corresponding to the alphabet we find in the differential equations. For PBmzm, we find that `Baikovletter` identifies one odd letter that is in fact not required. For PBzzm, the code does

---

[1]Following the completion of this work, a new version of `Baikovletter` was released, capable of identifying the missing letters, with the exception of the one in eq. (3.14). The latter requires analyzing a next-to-minimal Baikov representation, rather than the minimal representation used by `Baikovletter`. We thank Xuhang Jiang for correspondence on this matter.
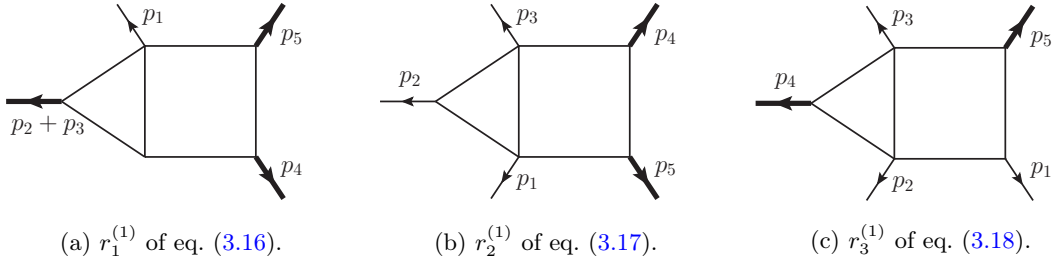
(a) $r_1^{(1)}$ of eq. (3.16). (b) $r_2^{(1)}$ of eq. (3.17). (c) $r_3^{(1)}$ of eq. (3.18).

Figure 3: Representative diagrams that introduce square roots.

not identify one of the square roots, which appears as the leading singularity of one of our pure integrals (a permutation of the one given in eq. (3.18) below, see also fig. 3c), and thus also misses the associated odd letters. We constructed four letters of the type given in eq. (3.12) that involve only that square root, as well as two letters of the type given in eq. (3.13), one involving the new root and $\sqrt{\lambda(s_4, s_{23}, s_{15})}$, and one involving the new root and $\sqrt{\Delta_5}$. One of the odd letters identified by the code is not required. Finally, `Baikovletter` misses sixteen letters for PBzmz. Fourteen out of these sixteen letters are related to the letters that are missed for PBzzm. These are two permutations of the square root given by eq. (3.18) below, and the associated twelve odd letters (six for each root) described above. The rational letter

$$s_4 s_{12} s_{15} + s_5 s_{23} s_{34} - s_{15} s_{34} s_{45} \tag{3.14}$$

is also not identified, even though it is a permutation of a rational letter that is identified. The last missed letter is odd in $\sqrt{\Delta_5}$, and the derivative of its logarithm is singular when the rational letter in eq. (3.14) vanishes, which presumably explains why it is not identified.

The representative families of fig. 2 correspond to a particular ordering of the external momenta. When computing a physical process, all permutations of massless and massive legs may appear. In order to obtain the full alphabet required for planar five-point two-mass processes at two loops, we must thus consider the closure of the alphabets discussed above under all such permutations.

As already highlighted, square roots play a distinguished role in building the alphabet, allowing us to classify the letters into even and odd letters depending on their charge under the change of the square-root sign. In order to organise our alphabet, we start by noticing that all square roots can be grouped into five permutation orbits.[2]

The first is the (square-root of) Källén function, and we take as a representative

$$\Delta_3^{(1)} = \lambda(s_4, s_5, s_{45}). \tag{3.15}$$

It can appear in 7 permutations $\Delta_3^{(i)}$, $i = 1, \ldots, 7$ (note the minus sign difference between the definition of Δ_3 in eq. (2.4) and $\Delta_3^{(i)}$). The second root appears as the leading singularity of the integral in fig. 3a with unit numerator, and its argument is

$$r_1^{(1)} = s_4^2 s_{23}^2 - 2 s_4 s_{23} (2 s_5 - s_{15} + s_{23}) s_{45} + (s_{15} - s_{23})^2 s_{45}^2, \tag{3.16}$$

and it can appear in 18 permutations $r_1^{(i)}$, $i = 1, \ldots, 18$. This root is associated with four-point three-mass kinematics, and was already identified in ref. [28]. The third root appears as the leading

---

[2]Note that this requires viewing five-point two-mass kinematics as a seven-point massless process, and then considering all permutations of the seven-point process that are consistent with five-point two-mass kinematics. Considering only the permutations of the massless momenta $\{p_1, p_2, p_3\}$ and the massive momenta $\{p_4, p_5\}$ would miss some relations.

Root	Degree	Orbit length
$\Delta_3^{(i)}$	2	7
Δ_5	4	1
$r_1^{(i)}$	4	18
$r_2^{(i)}$	4	6
$r_3^{(i)}$	4	12

(a) Polynomial degrees and permutation orbit lengths of the square roots appearing in the alphabet.

	$\Delta_3^{(i)}$	Δ_5	$r_1^{(i)}$	$r_2^{(i)}$	$r_3^{(i)}$
$\Delta_3^{(i)}$	38				
Δ_5	8	69			
$r_1^{(i)}$	36	30	66		
$r_2^{(i)}$	6	6	0	24	
$r_3^{(i)}$	12	12	0	0	48

(b) The number of letters that are odd in the square roots given in each row and column.

Table 2: Summary of the algebraic part of the alphabet, which contains 44 square roots and 355 algebraic letters.

singularity of the integral in fig. 3b with unit numerator, its argument is

$$r_2^{(1)} = s_4^2 s_{12}^2 + 2s_4 s_{12}(s_5 s_{23} + (s_{15} - s_{34})s_{45}) + (s_5 s_{23} + (s_{34} - s_{15})s_{45})^2 \,, \tag{3.17}$$

and it can appear in 6 permutations $r_2^{(i)}$, $i = 1, \ldots, 6$. The fourth root appears as the leading singularity of the integral in fig. 3c with unit numerator, its argument is

$$r_3^{(1)} = 4s_4 s_{12}(s_5 - s_{15})s_{15} + (s_5(s_{23} + s_{34}) - s_{15}(s_{34} + s_{45}))^2 \,, \tag{3.18}$$

and it can appear in 12 permutations $r_3^{(i)}$, $i = 1, \ldots, 12$. This square root can be computed in a very similar way as the Σ_5 square root was computed in [31]. As mentioned previously, it is missed by the `Baikovletter` code. It is however captured by the recursive Landau approach of [16]. The package `PLD.jl` [9] also detects it when computing Euler discriminants, but fails to detect it when computing principal Landau discriminants.[3] Finally, we also find the square-root of the five-point Gram determinant Δ_5,

$$\begin{aligned} \Delta_5 = {}& (s_4 s_{12} + s_{12}(s_{15} - s_{23}) + s_5 s_{23} - s_{23}s_{34} - s_{15}s_{45} + s_{34}s_{45})^2 - 4s_5 s_{12}s_{23}s_{34} \\ & - 4s_4 s_{12}(s_{12}s_{15} + (s_{15} - s_{34})(s_{23} - s_{45})) - 4s_{12}s_{23}s_{34}(s_{23} - s_{15} - s_{45}) \,, \end{aligned} \tag{3.19}$$

which is invariant under permutations. In total, this means that there are 44 roots for planar five-point two-mass scattering at two loops.

Let us now return to the closure of the letters in the alphabet under all permutations. We find that there is a total of 570 letters, out of which 215 are even and 355 are odd. Out of the odd letters, 236 are of the form in eq. (3.12) and depend on a single square-root and 119 are of the form in eq. (3.13) and depend on two square-roots (see table 2). The full alphabet can be found in our ancillary files.

3.3 Initial Conditions and Checks

In order to solve the differential equations we need the evaluation of the master integrals at a point. The package `AMFlow` [73, 74] makes this a triviality, and as such the determination of the initial conditions for the numerical solution of the differential equations is now a simple problem.

---

[3]We thank Mathieu Giroux and Sebastian Mizera for assistance in these checks. The failure of the principal Landau discriminant approach in identifying this singularity is related to the fact that one of the subloops is a triangle, whose leading singularity corresponds to taking the loop momentum to infinity and is a more subtle case to handle within this approach.

For completeness, we include in our ancillary files the numerical evaluation of our bases of integrals at a point in the Euclidean region (where integrals are either purely real or imaginary) and a point in what we call the 's_{12}-channel', corresponding to a process where p_1 and p_2 are in the initial state and p_3, p_4 and p_5 are in the final state (e.g., the production of two massive vector bosons together with a jet at a hadron collider). We refer the reader to appendix B for more details on how these kinematic regions are defined, and here simply quote the point we chose in the Euclidean region,

$$X_{\text{eu}} = \left(-\frac{3}{2}, -3, -\frac{57}{8}, -\frac{23}{4}, -\frac{5}{8}, -11, -1 \right) , \tag{3.20}$$

and the point in the s_{12}-channel,

$$X_0 = \left(7, -1, 2, 5, -2, 1, 1 \right) . \tag{3.21}$$

We note that the point X_{eu} is randomly chosen, but we verified that it does not correspond to a singular point of the differential equations. On the other hand, X_0 is chosen to be a good initial condition for the construction of pentagon functions according to the criteria of ref. [37]. In particular, aside from being in the s_{12}-channel kinematic region, it is symmetric under the external-momenta index swaps $1 \leftrightarrow 2$ and $4 \leftrightarrow 5$, which implies that it lies on the surface where $s_4 = s_5$.

The evaluations at these two points were obtained with 80-digit precision using `AMFlow`. We verified that, starting from X_{eu} and evolving the differential equations to X_0 with `DiffExp` [75] we obtain the same results. Given that X_0 is a very constrained kinematic point, we also evaluated the functions at a generic point X_1 in the s_{12}-channel,

$$X_1 = \left(\frac{7}{2}, -\frac{15}{53}, \frac{11}{8}, \frac{15}{17}, -\frac{7}{30}, \frac{1}{15}, \frac{4}{31} \right) . \tag{3.22}$$

Once again, we find complete agreement with the `AMFlow` evaluations and the `DiffExp` results obtained by using either X_0 or X_{eu} as an initial condition.[4]

Finally, solving the differential equations up to order ϵ is particularly simple (all integrals are normalised to start at order ϵ^0). One must simply require that the solutions to the differential equations only have logarithmic singularities at the physical thresholds, which amounts to imposing the so-called first entry condition [76]. In our case, the physical thresholds are at $s_4 = 0$, $s_5 = 0$ and $s_{ij} = 0$ if and only if the indices i and j correspond to external momenta appearing next to each other in the graph representing each family (see figs. 1 and 2). This fixes the solutions at order ϵ^0, which are just rational numbers. At order ϵ, the solutions are obtained from the differential equation as linear combinations of $\log(-s_4 - \mathrm{i}0^+)$, $\log(-s_5 - \mathrm{i}0^+)$ and $\log(-s_{ij} - \mathrm{i}0^+)$, where 0^+ is a positive infinitesimal, and i and j satisfy the conditions above. We compared the analytic solutions determined in this way to the numerical evaluations described above and found complete agreement.

3.4 Iterated Integral Solution

While in the previous section we solved the differential equations numerically, their canonical form also allows us to write the solution analytically in terms of Chen iterated integrals [2]. Order by

---

[4]We note that when evolving the solution from X_{eu} to X_1 with `DiffExp` for Pb, PBmzm and PBzmz we encounter a logarithmic singularity that cannot be analytically continued through by simply providing a positive imaginary part to s_{12}, s_{23}, s_{34}, s_{45}, s_{15}, s_4 and s_5 as one might have expect. The singularity is associated with the letter $s_4(s_5 - s_{34}) + s_{34}(s_{34} + s_{45} - s_5 - s_{12})$ and occurs outside of the physical s_{12} channel. To bypass this issue we can first evolve from X_{eu} to X_0 and then from X_0 to X_1, finding agreement with the `AMFlow` result. Within `DiffExp`, this result can be reproduced by giving the letter above a small negative imaginary part.

order in ϵ, we write the expansion of the master integrals as

$$\vec{I}_F(X, \epsilon) = \sum_{w \geq 0} \epsilon^w \, \vec{I}_F^{(w)}(X) \,. \tag{3.23}$$

At each order, the solution of the DE is then given by

$$\vec{I}_F^{(w)}(X) = \sum_{w'=0}^{w} \sum_{i_1, i_2, \ldots, i_{w'}} a_{i_1}^{(F)} \cdot a_{i_2}^{(F)} \cdots a_{i_{w'}}^{(F)} \cdot \vec{I}_F^{(w-w')}(X_0) \left[W_{i_{w'}}, \ldots, W_{i_2}, W_{i_1} \right]_{X_0}(X) \,, \tag{3.24}$$

where the sum in $i_1, i_2, \ldots, i_{w'}$ runs over the indices of all letters of the alphabet which are relevant for family F, $\vec{I}_F^{(w-w')}(X_0)$ are the initial values, and $\left[W_i, \ldots \right]_{X_0}(X)$ are the iterated integrals. The latter are defined iteratively as

$$\left[W_{i_1}, \ldots, W_{i_n} \right]_{X_0}(X) := \int_0^1 \mathrm{d}t \, \frac{\partial \log \left[W_{i_n}(\gamma(t)) \right]}{\partial t} \left[W_{i_1}, \ldots, W_{i_{n-1}} \right]_{X_0}(\gamma(t)) \,, \tag{3.25}$$

starting from $\left[\, \right]_{X_0}(X) := 1$. Here, γ is an arbitrary path in the space of kinematic variables X connecting the initial and the target point, i.e., $\gamma(0) = X_0$ and $\gamma(1) = X$. The number of iterated integrations, n in eq. (3.25), is called transcendental weight. Setting to zero all initial values with weight greater than 0 in eq. (3.25) ($\vec{I}_F^{(w)}(X_0) = 0$ for $w > 0$) removes the dependence on the initial point X_0 and yields the symbol of the solution [69]. This formalism is the starting point in the construction of a basis of special functions to express the solution [31, 36, 37, 77–79] and enables the study of its analytic properties. We refer to the review [5] for a thorough discussion, and limit ourselves to mention two properties which we will make use of in the next section. First, the algebraic independence of the letters W_i implies that iterated integrals with different sets of letters are $\mathbb{Q}$-linearly independent. This enables explicit cancellations and simplifications in analytic expressions, such as the cancellation of the poles at $\epsilon = 0$ in the double Lagrangian insertion computed in the next section. Second, the right-most entry of an iterated integral encodes the information about its derivatives. In particular, the definition in eq. (3.25) implies that

$$\mathrm{d}\left[W_{i_1}, \ldots, W_{i_n} \right]_{X_0}(X) = \mathrm{d}\log W_{i_n}(X) \left[W_{i_1}, \ldots, W_{i_{n-1}} \right]_{X_0}(X) \,. \tag{3.26}$$

We can then construct differential equations directly for the ($\mathbb{Q}$-linear combinations of) iterated integrals appearing in the result — say, for the double Lagrangian insertion computed in the next section — and solve them numerically, e.g., with `DiffExp`. This allows us to sidestep the more expensive evaluation of the master integrals when evaluating a result obtained from them [78].

4 Wilson Loop with Two Lagrangian Insertions

The families of two-loop integrals studied in this paper are indispensable for calculating many physically relevant quantities, such as QCD corrections to electroweak production processes. Here we provide a more modest application of one of the two-loop families (namely family PBmzz, see fig. 2) in the world of maximally super-symmetric Yang-Mills (sYM) theory. As compared to QCD amplitudes, the analytic structure of amplitudes and correlation functions in the $\mathcal{N} = 4$ sYM theory is usually restricted, which makes this theory a perfect testing ground for new results, allowing us to check if the integrals we have computed reproduce the expected properties of the theory.

The finite gauge-invariant quantity we are going to calculate is not an amplitude, and is naturally defined in coordinate space. Let us consider a Wilson loop W_{F} in the fundamental representation of the colour group $SU(N_c)$, defined as

$$W_{\mathrm{F}} = \frac{1}{N_c} \mathrm{tr} \, \mathrm{P} \exp \left(\mathrm{i} \, g_{\mathrm{YM}} \oint_C A_\mu(x) \mathrm{d}x^\mu \right) \,. \tag{4.1}$$

Here, $A_\mu(x) = A_\mu^a(x)\, t^a$ is a gauge field, where t^a are the generators of $SU(N_c)$ in the fundamental representation, and P stands for the path ordering of the colour indices. We take the simplest non-trivial contour C, that is a quadrilateral formed by four cusps with coordinates x_1, x_2, x_3, x_4, with all edges lying on the light cone, i.e.

$$x_{12}^2 = x_{23}^2 = x_{34}^2 = x_{14}^2 = 0\,, \tag{4.2}$$

where $x_{ij}^\mu := (x_i - x_j)^\mu$. We refer to eq. (4.1) with the light-like geometry of the contour as a *null Wilson loop*. The simplest nontrivial gauge-invariant quantity involving W_{F} one could consider is its vacuum expectation value, denoted $\langle W_{\mathrm{F}} \rangle$, and throughout this paper we will consider it in the planar limit where $N_c \to \infty$. Despite the ultra-violet finiteness of the $\mathcal{N} = 4$ sYM theory, $\langle W_{\mathrm{F}} \rangle$ is divergent owing to short-distance integrations in the vicinities of the cusps which require a regulator [80–82].

The dimensionally-regulated $\langle W_{\mathrm{F}} \rangle$ is well-known to coincide with the four-gluon Maximally Helicity Violating (MHV) amplitude, both at weak [42] and strong coupling [41], upon identification of the light-like momenta of the gluons ($q_i^2 = 0$) with the edges of the Wilson loop,

$$q_1 = x_{12}\,, \qquad q_2 = x_{23}\,, \qquad q_3 = x_{34}\,, \qquad q_4 = x_{41}\,. \tag{4.3}$$

The coordinates x_i are then called dual momenta (or region momenta) of the amplitude. The null Wilson loops are known to capture infrared divergences of amplitudes [83, 84] in a gauge theory. In the case of $\mathcal{N} = 4$ sYM, the duality not only maps between infrared divergences of the amplitude and cusp divergences of the null Wilson loop, but also identifies their finite parts.

The equivalence between null Wilson loops and MHV amplitudes also holds at the level of their four-dimensional integrands [85–87], which do not require a regulator. The Lagrangian-insertion procedure [88] provides a consistent definition of the four-dimensional Wilson loop integrand. It relies on the observation that, upon a suitable rescaling of the fields (e.g. $A_\mu \to 1/g_{\mathrm{YM}} A_\mu$), differentiation of the correlation function $\langle W_{\mathrm{F}} \rangle$ with respect to the coupling constant results in a new correlation function involving the Lagrangian of the theory [85]. In other words, the l-loop integrand of $\langle W_{\mathrm{F}} \rangle$, which we denote by $M^{(l)}(y_1, \ldots, y_l)$, is given by the correlation function of W_{F} and $\mathcal{N} = 4$ sYM Lagrangians $\mathcal{L}$ located at $y_1, \ldots, y_l$, which is to be calculated at the lowest perturbative order, i.e. $(g_{\mathrm{YM}}^2)^l$,

$$M^{(l)}(y_1, \ldots, y_l) := \langle W_{\mathrm{F}}\, \mathcal{L}(y_1) \ldots \mathcal{L}(y_l) \rangle_{(g_{\mathrm{YM}}^2)^l}\,. \tag{4.4}$$

Strictly speaking, $\mathcal{L}$ is the so-called *chiral on-shell* form of the Lagrangian, whose classical dimension is protected from quantum corrections by the superconformal symmetry. The expression of $\mathcal{L}$ in terms of fields of the theory and more details can be found in [89]. In fig. 4 we present examples of Feynman diagrams contributing to eq. (4.4) in the cases of one and two Lagrangian insertions. We stress that the correlator in the RHS of eq. (4.4) is finite in four space-time dimensions only at leading order in the coupling. The higher order corrections, which are not relevant for eq. (4.4), would require a regulator.

Thanks to the duality above, $M^{(l)}$ is a four-dimensional l-loop integrand of both $\langle W_{\mathrm{F}} \rangle$ and the MHV amplitude.[5] From the amplitude point of view, the integrand in eq. (4.4) is written in terms of dual momenta. The conformal symmetry of the Wilson-loop integrand thus translates into the dual-conformal symmetry of the amplitude's integrand. Integrating out the coordinates of one or several Lagrangian operators on the right-hand side of eq. (4.4) produces cusp divergences. Equivalently, performing the loop integrations in the corresponding integrand of the MHV amplitude leads to infrared divergences.

---

[5]More precisely, we are talking about colour-ordered MHV amplitudes normalised by their tree-level approximation, so that the integrand does not carry any colour nor helicity.
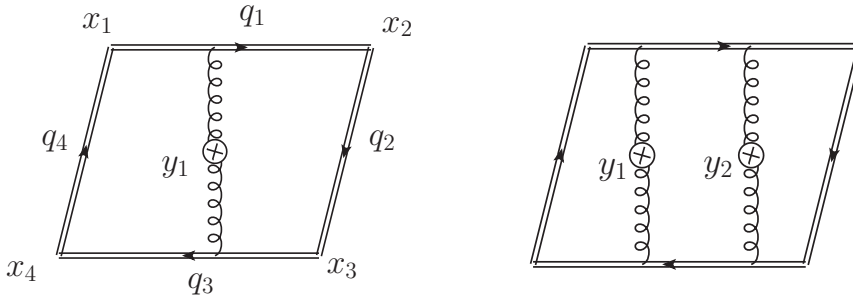
Figure 4: Typical Feynman diagrams representing the leading order contributions of the single ($l = 1$) and double ($l = 2$) Lagrangian insertions in the Wilson loop (see eq. (4.4)) are depicted on the left and right, respectively.

This motivates us to extend eq. (4.4) beyond the leading order of perturbation theory, and to define the following ratio of correlation functions,

$$F_l(x_1, \ldots, x_4; y_1, \ldots, y_l) := \frac{\pi^{2l}}{\langle W_{\mathrm{F}} \rangle} \langle W_{\mathrm{F}} \, \mathcal{L}(y_1) \ldots \mathcal{L}(y_l) \rangle . \tag{4.5}$$

As compared to eq. (4.4), where the perturbative expansion is truncated at the leading order, we are interested in higher orders in the expansion of eq. (4.5) in the coupling. The correlators in the numerator and denominator of eq. (4.5) are both divergent. These divergences originate from gluon exchanges in the vicinities of the Wilson loop cusps, but they cancel out in the ratio. Therefore, F_l is a finite quantity, well-defined in four space-time dimensions.

F_l has the same kinematics as the l-loop integrand $M^{(l)}$ defined in eq. (4.4), but we do not aim to integrate over any of the y_i in eq. (4.5), since such integrations are not well-defined in four space-time dimensions. As we motivate below, this gauge-invariant quantity, depending on both on-shell and off-shell variables, is of interest on its own. The perturbative expansion of F_l at weak coupling $g^2 := g_{\mathrm{YM}}^2 N_c / (16\pi^2)$ starts at order $(g^2)^l$,

$$F_l = \sum_{L \geq 0} (g^2)^{l+L} F_l^{(L)} . \tag{4.6}$$

The lowest order term is the l-loop integrand of the Wilson loop, $F_l^{(0)} = M^{(l)}$, see eq. (4.4). In what follows, when talking about L-loop corrections of F_l, we mean that L loop integrations are carried out.

The kinematic dependence of F_l is restricted by the conformal symmetry acting in the coordinate space. Indeed, the light-like contour of W_{F} is covariant upon conformal transformations, the scaling dimension of the Lagrangian does not receive quantum corrections, and the beta-function of the theory vanishes. Given the cancellation of cusp divergences in the ratio on the right-hand side of eq. (4.5), it follows that F_l is exactly conformal in four dimensions with respect to the cusp coordinates. However, F_l carries conformal weight $(+4)$ at the Lagrangian points. It is thus convenient to extract a factor which carries the nonzero conformal weights of F_l and multiplies a nontrivial function of conformal cross-ratios. We choose this prefactor to be $(x_{13}^2 x_{24}^2)^l \prod_{i=1}^{4} \prod_{j=1}^{l} (x_i - y_j)^{-2}$. Up to this normalization, F_l depends on the kinematics non-trivially only through $1 + (l-1)(l+6)/2$ conformal cross-ratios built from Lagrangian coordinates and cusps of the light-like contour.

In addition to conformal symmetry, F_l exhibits also a discrete symmetry: the dihedral transformations of the Wilson-loop contour. This means that F_l is invariant upon the cyclic shift of

all coordinates ($x_i \to x_{i+1}$ for all $i = 1, \ldots, 4$, with $x_{i+4} \equiv x_i$) and the inversion of their order ($x_i \to x_{5-i}$ for all $i = 1, \ldots, 4$).

Another way to understand the finiteness of F_l is to invoke the logarithm of the Wilson loop, $\log(\langle W_F \rangle)$, which has improved short-distance behaviour as compared to $\langle W_F \rangle$: the cusp divergences of $\langle W_F \rangle$ exponentiate, and $\log(\langle W_F \rangle)$ features only a one-loop divergence governed by the cusp Γ_{cusp} and collinear anomalous dimensions. For example, for the leading pole we have that $\log(\langle W_F \rangle) \propto \Gamma_{\text{cusp}}/\epsilon^2$. Differentiating l times $\log(\langle W_F \rangle)$ with respect to the coupling g^2 results in the insertion of l Lagrangians, e.g.

$$
\begin{aligned}
g^2 \partial_{g^2} \log(\langle W_F \rangle) &= \int \frac{\mathrm{d}^d y}{\mathrm{i}\,\pi^{\frac{d}{2}}} \, F_{l=1}(y)\,, \\
g^4 \left(\partial_{g^2}\right)^2 \log(\langle W_F \rangle) &= \int \frac{\mathrm{d}^d y_1}{\mathrm{i}\,\pi^{\frac{d}{2}}} \frac{\mathrm{d}^d y_2}{\mathrm{i}\,\pi^{\frac{d}{2}}} \, [F_{l=2}(y_1, y_2) - F_{l=1}(y_1) F_{l=1}(y_2)]\,,
\end{aligned}
\tag{4.7}
$$

et cetera. In other words, we can think of F_l as the integrand of $\log(\langle W_F \rangle)$ (up to products of F_m with $m < l$) where all but l loop integrations are carried out. More explicitly, $F_l^{(L)}$ results from L loop integrations in an $(L + l)$-loop rational four-dimensional integrand. The integrands in eq. (4.7) are finite, and the divergence in $\log(\langle W_F \rangle)$ arises only upon carrying out the remaining loop integrations.

The case of a single Lagrangian insertion, $l = 1$, in the four-cusp Wilson loop has been extensively studied in the literature, both at strong [45] and at weak [46–48] coupling, and using the negative geometry decomposition [52, 53] of the loop corrections. Here we initiate the study of double Lagrangian insertion, $l = 2$, and calculate $F_{l=2}$ for the first time in the two-loop approximation $F_{l=2}^{(2)}$. We obtain the functional form of the one-loop result in terms of familiar one-loop polylogarithmic functions, whereas we provide an iterated integral expression at two loops. Before we proceed to the case $l = 2$, we briefly recall the available perturbative results for $F_{l=1}$ and some of its remarkable properties.

4.1 Single Lagrangian Insertion

Let us briefly review the structure of $F_{l=1}$ in perturbation theory. In the case of a single Lagrangian insertion in the four-cusp Wilson loop, the kinematics is especially simple. Due to the conformal symmetry, it depends non-trivially on the single conformal cross-ratio z that can be built from the Lagrangian coordinate x_0 and cusp coordinates $x_1, \ldots, x_4$,

$$
F_{l=1}(x_1, \ldots, x_4; x_0) = \frac{x_{13}^2 x_{24}^2}{x_{10}^2 x_{20}^2 x_{30}^2 x_{40}^2} \sum_{L \geq 0} (g^2)^{1+L} J^{(L)} \left(z := \frac{x_{24}^2 x_{10}^2 x_{30}^2}{x_{13}^2 x_{20}^2 x_{40}^2} \right).
\tag{4.8}
$$

Here, $J^{(L)}(z)$ are pure harmonic polylogarithms [90] of weight $2L$, and the overall rational prefactor is the one-loop MHV amplitude integrand. The first two orders [46] are given by

$$
J^{(0)} = -1\,, \qquad J^{(1)} = \log^2(z) + \pi^2\,.
\tag{4.9}
$$

The expressions of $J^{(2)}$ and $J^{(3)}$, of transcendental weights 4 and 6, respectively, can be found in refs. [47, 48]. The dihedral symmetry implies that

$$
J^{(L)}(z) = J^{(L)} \left(\frac{1}{z} \right).
\tag{4.10}
$$

Without loss of generality, we can choose the conformal frame $x_0 \to \infty$ by means of a conformal transformation. Then, $z = x_{24}^2/x_{13}^2$ and, after identifying cusp coordinates with momenta according to eq. (4.3), we see that $z = t/s$ is the dimensionless ratio of the bi-particle Mandelstam variables,

$$
s = (q_1 + q_2)^2 \equiv x_{13}^2\,, \qquad t = (q_2 + q_3)^2 \equiv x_{24}^2\,.
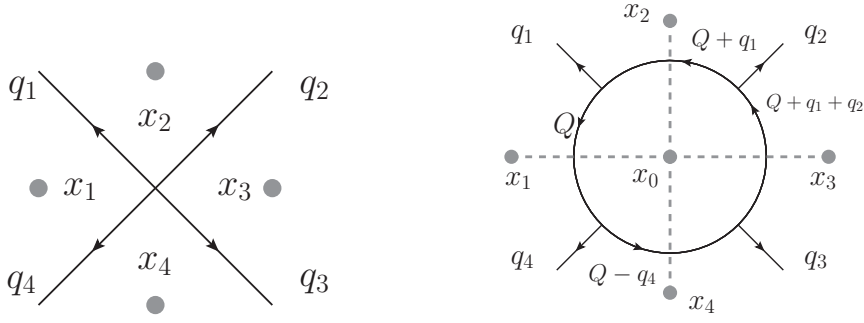\tag{4.11}
$$

Figure 5: Kinematics of the single (left) and double (right) Lagrangian insertions in the conformal frame, see eqs. (4.11) and (4.15), where one of the Lagrangians is located at infinity. Momenta and dual-momentum variables (see eq. (4.3)) correspond to dual graphs shown on the same picture. The arrows denote the directions of the momenta, the bullets denote the dual-momentum variables.

In other words, the loop corrections $J^{(L)}$ have the same kinematics as four-particle massless amplitudes. This correspondence is represented pictorially in fig. 5. Moreover, according to the conjecture in ref. [49], $J^{(L)}$ coincides with the part of maximal transcendental weight of the planar $(L+1)$-loop all-plus helicity amplitude in pure Yang-Mills theory (up to an overall normalisation factor).

Another remarkable observation about available perturbative data made in [52] is that they do not change sign in the anti-Euclidean region $s, t > 0$, namely at $z > 0$, but their sign alternates with the loop order,

$$(-1)^{L+1} J^{(L)}(z) > 0, \qquad \text{at} \quad z > 0. \tag{4.12}$$

We note that working in the anti-Euclidean region is conventional, and the same result holds in the Euclidean region $s, t < 0$.

4.2 Double Lagrangian Insertion

The kinematics of the double Lagrangian insertion in the four-cusp Wilson loop $F_{l=2}$ is much richer as compared to the $l = 1$ case shown in eq. (4.8). The conformal symmetry implies that $F_{l=2}$ is a nontrivial function of five conformal cross ratios, $\mathbf{z} := (z_1, \ldots, z_5)$, built from two Lagrangian coordinates $(x_0, x_{0'})$ and four cusp coordinates $(x_1, \ldots, x_4)$,

$$F_{l=2}(x_1, \ldots, x_4; x_0, x_{0'}) = \frac{x_{13}^2 x_{24}^2}{x_{10}^2 x_{20}^2 x_{30}^2 x_{40}^2} \frac{x_{13}^2 x_{24}^2}{x_{10'}^2 x_{20'}^2 x_{30'}^2 x_{40'}^2} \sum_{L \geq 0} (g^2)^{2+L} G^{(L)}(\mathbf{z}). \tag{4.13}$$

There is some freedom in choosing the five independent cross-ratios. In the following, we switch to the conformal frame $x_{0'} \to \infty$, and use the following set:

$$\mathbf{z} := \left(\frac{x_{10}^2 x_{30'}^2}{x_{13}^2 x_{00'}^2}, \frac{x_{20}^2 x_{10'}^2 x_{30'}^2}{x_{13}^2 x_{20'}^2 x_{00'}^2}, \frac{x_{30}^2 x_{10'}^2}{x_{13}^2 x_{00'}^2}, \frac{x_{40}^2 x_{10'}^2 x_{30'}^2}{x_{13}^2 x_{40'}^2 x_{00'}^2}, \frac{x_{24}^2 x_{10'}^2 x_{30'}^2}{x_{13}^2 x_{20'}^2 x_{40'}^2} \right) \xrightarrow{x_{0'} \to \infty} \left(\frac{x_{10}^2}{x_{13}^2}, \frac{x_{20}^2}{x_{13}^2}, \frac{x_{30}^2}{x_{13}^2}, \frac{x_{40}^2}{x_{13}^2}, \frac{x_{24}^2}{x_{13}^2} \right). \tag{4.14}$$

In order to translate the latter kinematic variables into amplitude language, we identify x_0^μ with an off-shell momentum Q^μ, e.g. we define $Q^\mu := x_{01}^\mu$ with $Q^2 \neq 0$. Together with the definition of the dual momenta in eq. (4.3), this implies that

$$x_{10}^2 = Q^2, \quad x_{20}^2 = (Q + q_1)^2, \quad x_{30}^2 = (Q + q_1 + q_2)^2, \quad x_{40}^2 = (Q - q_4)^2. \tag{4.15}$$

We represent this identification pictorially in fig. 5. In other words, $G^{(L)}$ in eq. (4.13) has the same kinematic dependence as the one-loop integrand of a massless four-particle amplitude. However, contrary to the usual one-loop integrands, $G^{(L)}$ is not rational beyond the leading order, namely for $L \geq 1$.

In this work, we calculate $G^{(L)}$ at $L = 0, 1, 2$. In order to achieve this goal, we need an efficient way to construct the loop integrands of $F^{(L)}_{l=2}$ in eq. (4.5). The four-dimensional integrands are sufficient for our goals since the loop integrations do not introduce divergences. As the integrands of the Wilson loops are identical to those of the MHV amplitudes, they can be easily obtained from the literature [91, 92]. Moreover, the L-loop integrand of the Wilson loop with l Lagrangian insertions is the $(l + L)$-loop MHV amplitude integrand. Then, calculating the ratio in eq. (4.5), we find that the loop integrand of $F^{(L)}_{l=2}$ is a combination of MHV amplitude loop integrands up to order $2 + L$. Explicitly, we have that[6]

$$F^{(0)}_{l=2}(x_0, x_{0'}) = M^{(2)}(x_0, x_{0'}),\qquad(4.16)$$

$$F^{(1)}_{l=2}(x_0, x_{0'}) = \int \frac{\mathrm{d}^4 y}{\mathrm{i}\,\pi^2} \left[M^{(3)}(x_0, x_{0'}, y) - M^{(1)}(y) M^{(2)}(x_0, x_{0'}) \right],\qquad(4.17)$$

$$\begin{aligned} F^{(2)}_{l=2}(x_0, x_{0'}) = \frac{1}{2} \int \frac{\mathrm{d}^4 y_1}{\mathrm{i}\,\pi^2} \frac{\mathrm{d}^4 y_2}{\mathrm{i}\,\pi^2} \Big[& M^{(4)}(x_0, x_{0'}, y_1, y_2) - 2 M^{(1)}(y_1) M^{(3)}(x_0, x_{0'}, y_2) \\ & - M^{(2)}(x_0, x_{0'}) M^{(2)}(y_1, y_2) + 2 M^{(1)}(y_1) M^{(1)}(y_2) M^{(2)}(x_0, x_{0'}) \Big], \end{aligned}\qquad(4.18)$$

where we recall that $M^{(L)}$ denotes the L-loop integrand of the MHV amplitude in eq. (4.4), and we omit the dependence on the cusp coordinates for the sake of compactness.

At the lowest order, $L = 0$, we see from eq. (4.16) that $F^{(0)}_{l=2}$ coincides with the two-loop integrand of the MHV amplitude. With the normalisation and expansion shown in eq. (4.13), in the frame $x_{0'} \to \infty$, we obtain

$$G^{(0)} = \frac{1}{x_{13}^2 x_{24}^2} \left[x_{13}^2 (x_{20}^2 + x_{40}^2) + x_{24}^2 (x_{10}^2 + x_{30}^2) \right],\qquad(4.19)$$

which can be rewritten in terms of the cross-ratios defined in eq. (4.14) as

$$G^{(0)}(\mathbf{z}) = z_1 + z_3 + \frac{z_2}{z_5} + \frac{z_4}{z_5} =: r_1(\mathbf{z}).\qquad(4.20)$$

Let us now move on to the loop corrections. First of all, in order to simplify the calculation, we eliminate one of the Lagrangian coordinates by choosing the conformal frame $x_{0'} \to \infty$ in the one-loop integrand in eq. (4.17). The loop integration in eq. (4.17) is well-defined in four space-time dimensions provided we do not break the integrand into the sum of smaller pieces and integrate them separately. Nonetheless, we find it convenient to adopt dimensional regularisation, so we can employ the usual amplitude workflow: we IBP-reduce the appearing scalar Feynman integrals to a basis of master integrals, and express them in terms of special functions. Then, the cancellation of the ϵ-poles of the individual master integrals is a strong self-consistency check of the calculation.

The kinematics of these Feynman integrals are however more constrained than in the usual momentum-space computations. Consider for example the two-mass pentagon Feynman integral with external momenta $p_1, \ldots, p_5$, whose kinematics is discussed in section 2.1. The map between the momenta of the integral (p_i) and those of the Lagrangian insertion (q_i) is given by

$$p_1 = x_{12} = q_1, \quad p_2 = x_{23} = q_2, \quad p_3 = x_{34} = q_3, \quad p_4 = x_{40} = q_4 - Q, \quad p_5 = x_{01} = Q,\quad(4.21)$$

as shown in fig. 6. The constraints in eq. (4.2) then imply that $p_1^2 = p_2^2 = p_3^2 = 0$, as in section 2.1. While p_4 and p_5 are off-shell, they are constrained by the fact that their sum must be light-like,

---

[6]See ref. [50] for an analogous derivation of the loop integrands in the case of the single Lagrangian insertion.
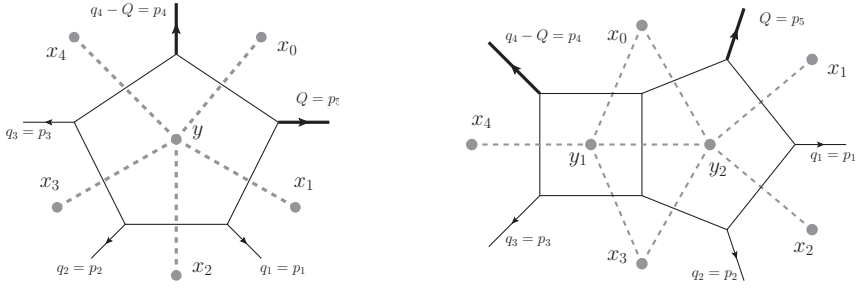
Figure 6: Two-mass pentagon and two-mass pentabox topologies contributing to the one- and two-loop integrand of the double Lagrangian insertion $F_{l=2}$. We interpose on the same figure the Feynman diagrams drawn in momentum and dual momentum variables. The solid lines represent propagators in momentum space. The dashed lines, connecting bullets, represent propagators in the dual momentum notation. We also identify the momenta of the integrands q_i with the momenta p_i in figs. 1 and 2 (see eq. (4.21)). The kinematics is constrained since $(p_4 + p_5)^2 = 0$.

since $p_4 + p_5 = x_{41} = q_4$. We then have an additional constraint on the Mandelstam variables X defined in eq. (2.2),

$$s_{45} = (p_4 + p_5)^2 = 0 \,. \tag{4.22}$$

As a result, instead of six dimensionless variables, only five are required ($z_1, \ldots, z_5$, defined in eq. (4.14)), and we find that $F_{l=2}^{(1)}$ in eq. (4.17) contains only the following one-loop Feynman integrals: the two-mass pentagon depicted in fig. 6 (as well as its dihedral permutations), boxes (with zero and two external masses at adjacent legs), triangles (with one, two, and three external masses), and bubbles.

By repeating this analysis for the two-loop integrand of $F_{l=2}^{(2)}$, we find that the most complicated Feynman integral topology that contributes is the two-mass pentabox PBmzz depicted in fig. 6, along with its dihedral permutations. As in the case of the two-mass pentagon, the kinematic dependence of the pentabox is restricted to five dimensionless variables by the constraint in eq. (4.22). The other contributing topologies are the double-boxes (with zero and two external massive legs attached to the same box) [93], and products of one-loop topologies.

In the previous sections we have derived the canonical differential equations and identified the symbol alphabet for the PBmzz family. We need to impose on them the additional constraint $s_{45} = 0$ required in the current calculation. This can be done straightforwardly through the differential equations. We write down the asymptotic solution of the canonical differential equations for PBmzz family in the $s_{45} \to 0$ limit by following the method of ref. [94] (see ref. [95] for an application to Feynman integrals). In doing this, one must take care that only the so-called 'hard region' of the asymptotic expansion is kept, which amounts to setting $s_{45} = 0$ at the integrand level (see ref. [96] for a thorough discussion of the method of regions). In order to remove from the asymptotic expansion all the other regions, we drop all terms which go as $s_{45}^{-a\epsilon+b}$, where a is a positive rational number and b is a non-negative integer, and then set $s_{45} = 0$. The resulting iterated integral representation of the PBmzz Feynman integrals at $s_{45} = 0$ involves a smaller alphabet.

The symbol of the two-mass pentabox PBmzz integrals (with the orientation of the external legs shown in fig. 2) in the full 7-variable kinematics of section 2.1 involves 80 letters of the 570-letter alphabet discussed in section 3.2. By taking the limit $s_{45} \to 0$, rewriting the resulting letters in the variables $\mathbf{z}$ defined in eq. (4.14) and including all dihedral permutations, we obtain an alphabet of

86 letters. Among them, there are 43 even and 43 odd (algebraic) letters which involve 11 square roots. We emphasise that this is not a sub-alphabet of the 570-letter alphabet from section 3.2.

We treat similarly the other contributing families. We use the canonical bases for the double-box families from [93] and re-derive their differential equations in terms of our 86-letter alphabet with the setup discussed in section 3. The identified 86-letter alphabet therefore captures the analytic structure of $F_{l=2}$ up to two loops. The one-loop approximation $F_{l=2}^{(1)}$ requires a 14-letter subalphabet involving only two square roots.

Finally, we find that the one- and two-loop coefficients of the double Lagrangian insertion in eq. (4.13) have the form

$$G^{(1)}(\mathbf{z}) = \sum_{i=1}^{7} r_i(\mathbf{z}) f_i^{(1)}(\mathbf{z}), \qquad G^{(2)}(\mathbf{z}) = \sum_{i=1}^{64} r_i(\mathbf{z}) f_i^{(2)}(\mathbf{z}), \qquad (4.23)$$

where the $r_i(\mathbf{z})$ are algebraic functions, while $f_i^{(1)}(\mathbf{z})$ and $f_i^{(2)}(\mathbf{z})$ are pure special functions of uniform transcendental weight two and four, respectively. Therefore, we observe that the double Lagrangian insertion $F_{l=2}$ satisfies the principle of maximal transcendentality [97] as one might have expected (we note that the same is true for the single Lagrangian insertion $F_{l=1}$). While we are only interested in the four-dimensional result here, we have also verified that the one- and two-loop corrections to the double Lagrangian insertion have uniform transcendental weight to all orders in ϵ by writing them as linear combinations of pure integrals multiplied by ϵ-independent coefficients

Among the 86 letters appearing in the two-loop Feynman integrals, there is one dihedral-invariant square-root letter which originates from Δ_5 in eq. (2.7) by setting $s_{45} = 0$,

$$\bar{\Delta}_5 := \mathrm{Gram}(x_{12}, x_{23}, x_{34}, x_{10}). \qquad (4.24)$$

We observe that letter $\bar{\Delta}_5$ drops out of the finite quantity $G^{(2)}(\mathbf{z})$. This is in line with previous observations about the cancellation of the analogous square-root letter Δ_5 from the finite remainders of five-particle massless and one-mass amplitudes. In the massless case, this phenomenon was linked to cluster algebras [98] and Gröbner fans [99].

As compared to the single Lagrangian insertion $F_{l=1}$, which requires just one rational prefactor (see eq. (4.8)), the double Lagrangian insertion has a more complicated structure. It involves 64 coefficients ($r_i(\mathbf{z})$ in eq. (4.23)), of which 28 are rational, and 36 are algebraic. The algebraic coefficients are normalised by one of the 11 square roots in the alphabet, and are otherwise rational. The double Lagrangian insertion is however independent of the choice of the branches of the square roots. Indeed, each algebraic coefficient is accompanied in eq. (4.23) by a pure function which is odd with respect to the sign of the corresponding square root, so that their product is even. Furthermore, some coefficients contain spurious singularities, i.e., loci where some coefficients $r_i(\mathbf{z})$ diverge while $G^{(1)}(\mathbf{z})$ and $G^{(2)}(\mathbf{z})$ should stay finite. The spurious singularities come from polynomials in the denominators of $r_i(\mathbf{z})$ as well as from the square roots discussed above. We checked at symbol level that the spurious poles of $r_i(\mathbf{z})$ are suppressed by zeros of the accompanying pure functions $f_i^{(L)}(\mathbf{z})$, and expect this to hold at function level.

Despite this higher complexity, the analogy with the single Lagrangian insertion extends also to certain properties of the rational coefficients. As for the rational coefficient of the single Lagrangian insertion in eq. (4.8), in fact, we find that all the coefficients of the one- and two-loop double Lagrangian insertion in eq. (4.23) have unit leading singularities [3]. The leading singularities of an integrand are the residues at the singularities of the highest codimension in the integration variables. Denoting by $\mathrm{LS}_v [f]$ the leading singularities of an integrand f with integration variables v, for the rational coefficient of the single Lagrangian insertion (see eq. (4.8)) we have that

$$\mathrm{LS}_{x_0} \left[\frac{x_{13}^2 x_{24}^2}{x_{10}^2 x_{20}^2 x_{30}^2 x_{40}^2} \right] = 1. \qquad (4.25)$$

– 20 –

This is nothing but the translation into dual momenta of the well-known fact that the leading singularity of the massless one-loop box is $1/(st)$. We have verified by means of the package `DlogBasis` [24] that the same holds for the coefficients of the double Lagrangian insertion,[7]

$$\underset{x_0,x_{0'}}{\mathrm{LS}} \left[r_i(\mathbf{z}) \frac{x_{13}^2 x_{24}^2}{x_{10}^2 x_{20}^2 x_{30}^2 x_{40}^2} \frac{x_{13}^2 x_{24}^2}{x_{10'}^2 x_{20'}^2 x_{30'}^2 x_{40'}^2} \right] = \underset{x_0}{\mathrm{LS}} \left[r_i(\mathbf{z}|_{x_{0'} \to \infty}) \frac{x_{13}^2 x_{24}^2}{x_{10}^2 x_{20}^2 x_{30}^2 x_{40}^2} \right] = 1 \,. \qquad (4.26)$$

We stress that, for this property to hold, the overall rational normalisation factor carrying the conformal weights of the double Lagrangian insertion in eq. (4.13) needs to be kept into account as well. Conformal symmetry then allows us to simplify the computation by a transformation $x_0' \to \infty$ to the conformal frame. This property can be explained heuristically as follows. The coefficients $r_i(\mathbf{z})$ in eq. (4.23) can be obtained from $G^{(1)}(\mathbf{z})$ and $G^{(2)}(\mathbf{z})$ by taking discontinuities iteratively until all pure functions $f_i^{(L)}$ are replaced by powers of $i\pi$. These discontinuities correspond to suitable residues of the integrands of $F_{l=2}^{(1)}$ and $F_{l=2}^{(2)}$. The latter are built from loop integrands of MHV amplitudes $M^{(L)}$ (see eqs. (4.16) – (4.18)), which are known to admit a d log representation and have unit leading singularities [44, 100]. Since all residues of a d log form with unit leading singularities are themselves d log forms with unit leading singularities, we can expect that this property should hold for the coefficients $r_i(\mathbf{z})$.

Finally, we organised $G^{(1)}$ and $G^{(2)}$ in such a way that they are manifestly invariant under dihedral transformations of the kinematic variables. The latter in fact act by permuting the addends $r_i(\mathbf{z}) f_i^{(L)}(\mathbf{z})$ in the expressions of $G^{(1)}$ and $G^{(2)}$ given in eq. (4.23), thus leaving the sums invariant.

We provide analytic expressions for $G^{(1)}$ and $G^{(2)}$ in the ancillary files, together with the definition of the corresponding alphabet letters and of the algebraic coefficients $r_i(\mathbf{z})$. In the one-loop case we provide an explicit polylogarithmic representation for $\{f_i^{(1)}\}_{i=1}^7$. They are given by the zero-mass-box, two-mass-hard-box, and three-mass-triangle functions. In the two-loop case, we provide an iterated integral expression for $\{f_i^{(2)}\}_{i=1}^{64}$ with iterated integrals defined with respect to the base point

$$\mathbf{z}_0 \,:\, \left(x_{10}^2 = 1,\, x_{20}^2 = 1,\, x_{30}^2 = 3,\, x_{40}^2 = 3,\, x_{13}^2 = 1,\, x_{24}^2 = 1 \right). \qquad (4.27)$$

In order to evaluate them numerically, we follow the approach of ref. [78]: we derive the system of differential equations they satisfy, and solve them with the method of generalised power series expansions [101]. In other words, we construct the canonical system of differential equations

$$\mathrm{d}\vec{F}(\mathbf{z}) = \mathrm{d}A(\mathbf{z}) \cdot \vec{F}(\mathbf{z}), \qquad \mathrm{d} = \sum_{i=1}^{5} \mathrm{d}z_i \frac{\partial}{\partial z_i}, \qquad (4.28)$$

for 187 uniform-weight iterated integrals $\{F_i\}_{i=1}^{187}$. The first 64 are the weight-four iterated integrals appearing in $G^{(2)}$, i.e., $F_i = f_i^{(2)}$ for $i = 1, \ldots, 64$. The remaining ones (F_i for $i = 65, \ldots, 187$) are lower-weight iterated integrals which result from the iterative differentiation of $\{f_i^{(2)}\}_{i=1}^{64}$. The absence of the letter $\bar{\Delta}_5$ (4.24) is manifest in the connection matrix $\mathrm{d}A(\mathbf{z})$, which is written in terms of the other 85 letters. Finally, we obtained numerical boundary values $\vec{F}(\mathbf{z}_0)$ at the base point $\mathbf{z}_0$ with (at least) 55-digit precision by means of `AMFlow` [73, 74]. The canonical differential equations in eq. (4.28), supplemented by the boundary values, can then be integrated numerically. We make use of `DiffExp` [75] to evaluate numerically the two-loop double Lagrangian insertion, allowing us to investigate its positivity properties.

---

[7]Strictly speaking, these leading singularities are non-zero rational constants. The normalisation of the coefficients is however arbitrary, as these constants can be absorbed into the definition of the pure functions they multiply.

4.3 Uniform Sign of the Loop Corrections

The remarkable positivity property of the loop corrections to the single Lagrangian insertion (see eq. (4.12)) begs for a generalisation to the double Lagrangian insertion. We conjecture that the loop corrections to $F_{l=2}$ also have a uniform sign which alternates with the loop order, as

$$(-1)^L G^{(L)}(\mathbf{z}) > 0, \qquad \mathbf{z} \in \mathbb{A}, \tag{4.29}$$

in a special kinematic region $\mathbb{A}$ which is defined by the amplituhedron [51].

The double Lagrangian insertion suggests that we consider the two-loop four-particle MHV amplituhedron. This geometry is carved out by inequalities on the four-brackets of momentum twistors [102], which are translated to our space-time variables in the frame $x_{0'} \to \infty$ as follows:

$$\mathbb{A} \; : \; \begin{cases} x_{10}^2 > 0, \quad x_{20}^2 > 0, \quad x_{30}^2 > 0, \quad x_{40}^2 > 0, \quad x_{13}^2 > 0, \quad x_{24}^2 > 0, & (4.30) \\ x_{13}^2(x_{20}^2 + x_{40}^2) + x_{24}^2(x_{10}^2 + x_{30}^2) - x_{13}^2 x_{24}^2 > 0, \quad \bar{\Delta}_5 > 0. & (4.31) \end{cases}$$

The region $\mathbb{A}$ is thus a subregion of the anti-Euclidean region (see the comment below eq. (4.12)), which is defined by the inequalities in eq. (4.30), restricted by the constraints in eq. (4.31). We provide more details on this region in appendix B.

One can easily see that the lowest order correction in eq. (4.20) is positive, $G^{(0)}(\mathbf{z}) > 0$, in the whole Euclidean region. The amplituhedron constraints become relevant starting from one loop. In other words, while $G^{(1)}(\mathbf{z})$ does change sign within the Euclidean region, we observe that $G^{(1)}(\mathbf{z}) < 0$ inside the subregion $\mathbb{A}$. This is based on the evaluation of the polylogarithmic function $G^{(1)}(\mathbf{z})$ in $O(10^7)$ random points in $\mathbb{A}$. The negativity of $G^{(1)}(\mathbf{z})$ in $\mathbb{A}$, namely that a 5-variable polylogarithmic function does not change sign inside a curvy region $\mathbb{A}$, appears to be very nontrivial. Let us note that seven terms $\{r_i f_i\}_{i=1}^7$ in the expression for $G^{(1)}(\mathbf{z})$ given by eq. (4.23) do not have fixed sign inside $\mathbb{A}$, yet they conspire to guarantee that $G^{(1)}(\mathbf{z}) < 0$. In our numerical study, we detected $45 < 2^7 - 1$ different sign patterns $\{\mathrm{sign}(r_i f_i)\}_{i=1}^7$. Of course, this counting holds for our particular representation of the answer, and a rearrangement of terms in eq. (4.23) could potentially decrease the number of sign patterns.

The iterated integral expression for the two-loop correction allows us to evaluate $G^{(2)}$ numerically as well. Here we provide the benchmark values

$$G^{(0)}(\mathbf{z}_1) \approx 24.261630456, \quad G^{(1)}(\mathbf{z}_1) \approx -988.27502992, \quad G^{(2)}(\mathbf{z}_1) \approx 27222.154196, \tag{4.32}$$

at the random point

$$\mathbf{z}_1 \in \mathbb{A}: \quad \left(x_{10}^2 = \frac{271}{13}, \, x_{20}^2 = \frac{463}{29}, \, x_{30}^2 = \frac{499}{79}, \, x_{40}^2 = \frac{299}{83}, \, x_{13}^2 = \frac{73}{53}, \, x_{24}^2 = \frac{367}{89} \right). \tag{4.33}$$

We evaluated $G^{(2)}(\mathbf{z}_1)$ in two different ways. On the one hand, we evaluated numerically all Feynman integrals contributing to $G^{(2)}$ at $\mathbf{z} = \mathbf{z_1}$ using `AMFlow`, and once again observed the cancellation of the ϵ-poles coming from individual integrals. On the other hand, using `DiffExp`, we integrated numerically the canonical differential equation in eq. (4.28) satisfied by $\{f_i^{(2)}\}_{i=1}^{64}$, this way transporting their values from the base point $\mathbf{z} = \mathbf{z}_0 \in \mathbb{A}$ given in eq. (4.27) to $\mathbf{z} = \mathbf{z}_1$. We find agreement between the two evaluations within the expected numerical accuracy, which is an additional cross-check of our calculation. The second approach is advantageous, since it requires fewer computational resources. Indeed, it does not require dimensional regularisation, and directly provides the values of the transcendental functions $\{f_i^{(2)}\}_{i=1}^{64}$.

We would like to stress that *all* the amplituhedron constraints defining the region $\mathbb{A}$ in eqs. (4.30) and (4.31) are essential for the uniform sign conjecture to hold. Indeed, the sign is not uniform in

the whole anti-Euclidean region defined by eq. (4.30) alone. To see this, let us consider the following ray parametrised by $t > 0$,

$$\mathbf{z}_{\mathrm{E}}(t): \quad \left(x_{10}^2 = \frac{31}{4046}, x_{20}^2 = \frac{86}{663}, x_{30}^2 = \frac{3824}{2329}, x_{40}^2 = \frac{2858}{4159}, x_{13}^2 = t\frac{4741}{85}, x_{24}^2 = t\frac{4262}{79}\right),$$

which belongs to the anti-Euclidean region. This ray punctures the amplituhedron region $\mathbb{A}$ defined in eq. (4.31), as $\mathbf{z}_{\mathrm{E}}(t) \notin \mathbb{A}$ at $t \gtrsim 0.02817$ and $\mathbf{z}_{\mathrm{E}}(t) \in \mathbb{A}$ otherwise. We verify that the uniform sign conjecture of eq. (4.29) holds on the segment of the ray which is inside $\mathbb{A}$. However, the one-loop correction evaluated on the ray, $G^{(1)}(\mathbf{z}_{\mathrm{E}}(t))$, changes sign at $t \approx 1.34435$, while the change of sign for the two-loop correction $G^{(2)}(\mathbf{z}_{\mathrm{E}}(t))$ happens at $t \approx 0.45154$. In other words, the sign of the loop corrections is not uniform outside of the amplituhedron region $\mathbb{A}$.

We evaluated $G^{(2)}(\mathbf{z})$ at a number of points $\mathbf{z} \in \mathbb{A}$ with `DiffExp`, and found agreement with our positivity conjecture (see eq. (4.29)). More explicitly, we evaluated it along $\mathcal{O}(10)$ one-dimensional slices of the kinematics emanating from $\mathbf{z}_0$. Still, the current approach to the numerical evaluation of $G^{(2)}$ is not efficient enough to test the conjecture on a sample of the same size as we used in the one-loop case. It would be extremely interesting to undertake a more detailed study of the positivity of $G^{(2)}(\mathbf{z})$. Given that the analytic structure of $G^{(2)}(\mathbf{z})$ is much more complicated than that of $G^{(1)}(\mathbf{z})$, the expected positivity of $G^{(2)}(\mathbf{z})$ seems to be even more miraculous.

The four-dimensional amplitude integrands are differential forms with positive coefficients inside the amplituhedron geometry [103], which belong to an anti-Euclidean region. At the same, the alternating sign property of the loop corrections arises after integration over a Minkowski contour. Thus, it is not clear whether the positivity of the integrands can explain the uniform sign of the loop corrections. Our conjecture for the double Lagrangian insertion adds to a list of similar observations about positivity properties of the integrated loop corrections in the amplituhedron geometry, e.g. the finite ratio function of the six-particle amplitude [104], and the single Lagrangian insertion in the four-cusp [52] and five-cusp [50] null Wilson loops.

5 Conclusions

In this paper we constructed analytic differential equations for a complete set of planar two-loop five-point Feynman integrals with two off-shell external legs. There are six different two-loop integral families that do not factorise into products of one-loop integrals, and for each of them we have determined a pure basis, satisfying a differential equation in canonical form. The corresponding logarithmic forms were mostly obtained from newly developed tools that allow one to construct symbol letters. The analytic differential equations were then obtained from finite-field samples with techniques that are by now standard. We observed that, despite the large number of scales involved in these integrals, modern IBP-reduction tools were able to handle these calculations. The derived analytic differential equations can be readily solved through generalised power series expansions. This allowed us to perform consistency checks by transporting numerical solutions between the Euclidean region and a physical region, finding agreement with an independent evaluation through the auxiliary mass flow method.

The families we considered need to be closed under permutations to cover all integrals that appear in physical quantities such as amplitudes. With that observation in mind, we completed the alphabet with these transformations, finding a total of 570 letters. This is substantially larger than the alphabet for planar five-point scattering with a single off-shell external leg at two-loops (which has 58 letters). In particular, we observe a large increase in the number of square roots appearing in these differential equations compared to the one-mass case. Nevertheless, the analytic structure of the letters is similar to that observed in other five-point integrals involving several roots. This

observation gives us great confidence that the strategy to build pentagon functions established in ref. [31] will be directly applicable for this set of integrals. This is however left for future work.

In the second part of this paper, we used our integrals to initiate the study of the double Lagrangian insertion in the null Wilson loop in $\mathcal{N} = 4$ super-symmetric Yang-Mills. Our motivation was twofold. First, the analytic properties of quantities in $\mathcal{N} = 4$ sYM are very constrained, so recovering those expected properties with our integrals is a non-trivial check of their correctness. Second, we would like to understand which of the beautiful properties observed for the single Lagrangian insertions extend to the double Lagrangian insertions. Compared to the former, the kinematic space of the latter is multidimensional already for the simplest null-polygonal contour, the quadrilateral, which we considered in this paper. We confirmed the expectations that the double Lagrangian insertion is finite, conformally invariant in four dimensions, and has uniform transcendentality. The analytic structure is described by a 85-letter alphabet involving 11 square roots. The rational coefficients accompanying the pure functions are rather special as well, as they have unit leading singularities. We took the necessary steps required to numerically evaluate the double Lagrangian insertions up to two-loops, which allowed us to formulate and test a new conjecture on the positivity of these quantities inside a kinematic region defined by the amplituhedron.

There are however many open questions that remain to be answered about double Lagrangian insertions in a Wilson loop. For instance, with a view to a three-loop bootstrap, it would be interesting to understand whether the alphabet stabilises at two loops, and whether new rational coefficients can appear at higher loop orders. Another question we have not investigated is whether the hidden momentum-space conformal symmetry of the single Lagrangian insertion [49] has a counterpart for the double Lagrangian insertion. Also, we would like to understand whether the double Lagrangian insertion can be identified with any amplitude in non-supersymmetric theories, as is the case for the single Lagrangian insertion and the all-plus helicity amplitude in pure Yang-Mills theory [49]. The perturbative data we provide are a good starting point for these investigations, which we leave to future work.

Acknowledgments

A Pure Master Integrals for the Five-Point Sectors

In this appendix, we present our pure bases for all independent five-point sub sectors (modulo permutations of the external massless legs, and exchanges $p_4 \leftrightarrow p_5$). We omit those sectors whose integrals are products of one-loop integrals. Explicit, machine-readable expressions for all master integrals can be found in our ancillary files [58].

PBmmz, $\{1,1,1,1,1,1,1,1,0,0,0\}$, 3 MIs

$$\mathcal{N}^{(1)}_{\mathrm{PBmmz}} = \epsilon^4 \sqrt{\Delta_5}\,(p_1+p_2)^2\,\mu_{12}\,,$$
$$\mathcal{N}^{(2)}_{\mathrm{PBmmz}} = \epsilon^4 \sqrt{\Delta_5}\,(p_1+p_2)^2\,\mu_{22}\,,$$
$$\mathcal{N}^{(3)}_{\mathrm{PBmmz}} = \epsilon^4\,s_{12}(s_4 s_{12} - s_{34} s_{45})\,(k_2-p_1)^2\,. \tag{A.1}$$

PBmzm, $\{1,1,1,1,1,1,1,1,0,0,0\}$, 3 MIs

$$\mathcal{N}^{(1)}_{\mathrm{PBmzm}} = \epsilon^4 \sqrt{\Delta_5}\,(p_1+p_2)^2\,\mu_{12}\,,$$
$$\mathcal{N}^{(2)}_{\mathrm{PBmzm}} = \epsilon^4 \sqrt{\Delta_5}\,(p_1+p_2)^2\,\mu_{22}\,,$$
$$\mathcal{N}^{(3)}_{\mathrm{PBmzm}} = \epsilon^4\,s_{12}(s_4 s_5 - s_4 s_{34} - s_5 s_{34} - s_{12} s_{34} + s_{34}^2 + s_{34} s_{45})$$
$$\times\,(k_2-p_1)^2\,. \tag{A.2}$$

PBmzz, $\{1,1,1,1,1,1,1,1,0,0,0\}$, 3 MIs

$$\mathcal{N}^{(1)}_{\mathrm{PBmzz}} = \epsilon^4 \sqrt{\Delta_5}\,(p_3+p_4)^2\,\mu_{12}\,,$$
$$\mathcal{N}^{(2)}_{\mathrm{PBmzz}} = \epsilon^4 \sqrt{\Delta_5}\,(p_3+p_4)^2\,\mu_{22}\,,$$
$$\mathcal{N}^{(3)}_{\mathrm{PBmzz}} = \epsilon^4\,s_{12} s_{15}\left[s_{34}\,(k_2-p_3)^2 - s_4\,k_2^2\right]\,. \tag{A.3}$$

PBzmz, $\{1,1,1,1,1,1,1,1,0,0,0\}$, 3 MIs

$$\mathcal{N}^{(1)}_{\mathrm{PBzmz}} = \epsilon^4 \sqrt{\Delta_5}\,(p_2+p_4)^2\,\mu_{12}\,,$$
$$\mathcal{N}^{(2)}_{\mathrm{PBzmz}} = \epsilon^4 \sqrt{\Delta_5}\,(p_2+p_4)^2\,\mu_{22}\,,$$
$$\mathcal{N}^{(3)}_{\mathrm{PBzmz}} = \epsilon^4\,(s_4 s_{15} - s_4 s_5 + s_{12} s_{15} + s_5 s_{23} + s_5 s_{34}$$
$$-\,s_{15} s_{34} - s_{15} s_{45})\left[s_{24}\,(k_2-p_2)^2 - s_4\,k_2^2\right] \tag{A.4}$$

PBzzm, $\{1,1,1,1,1,1,1,1,0,0,0\}$, 3 MIs

$$\mathcal{N}^{(1)}_{\text{PBzzm}} = \epsilon^4 \sqrt{\Delta_5}\,(p_1 + p_4)^2\,\mu_{12}\,,$$
$$\mathcal{N}^{(2)}_{\text{PBzzm}} = \epsilon^4 \sqrt{\Delta_5}\,(p_1 + p_4)^2\,\mu_{22}\,,$$
$$\mathcal{N}^{(3)}_{\text{PBzzm}} = \epsilon^4\, s_{23}(s_4 + s_5 + s_{12} - s_{34} - s_{45})$$
$$\times \left[s_{14}\,(k_2 - p_1)^2 - s_4\,k_2^2 \right]\,. \tag{A.5}$$

PBzzz, $\{1,1,1,1,1,1,1,1,0,0,0\}$, 4 MIs

$$\mathcal{N}^{(1)}_{\text{PBzzz}} = \epsilon^4 \sqrt{\Delta_5}\,(p_4 + p_5)^2\,\mu_{12}\,,$$
$$\mathcal{N}^{(2)}_{\text{PBzzz}} = \epsilon^4 \sqrt{\Delta_5}\,(p_4 + p_5)^2\,\mu_{22}\,,$$
$$\mathcal{N}^{(3)}_{\text{PBzzz}} = \epsilon^4\, s_{45}\big[s_{12}s_{23}\,(k_2 - p_4)^2 - s_{12}s_{15}\,k_2^2$$
$$- s_{23}s_{34}\,(k_2 - p_4 - p_5)^2 \big]\,. \tag{A.6}$$

We took the definition of the forth MI from ref. [14]. Its normalisation involves the product of two square roots (of Δ_5 and $\lambda(s_4, s_5, s_{45})$). The expression is however lengthy and we thus omit it here.

PBmmz, $\{1,1,1,1,1,1,0,1,0,0,0\}$, 4 MIs
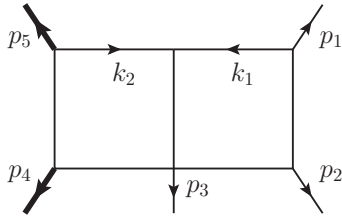
$$\mathcal{N}^{(4)}_{\text{PBmmz}} = \epsilon^4 \sqrt{\Delta_5}\,\mu_{12}\,,$$
$$\mathcal{N}^{(5)}_{\text{PBmmz}} = \epsilon^4 \sqrt{\lambda(s_4, s_5, s_{45})}\,s_{12}\,(k_2 - p_1)^2\,,$$
$$\mathcal{N}^{(6)}_{\text{PBmmz}} = \epsilon^4\, s_{12}(s_{23}s_5 - s_{15}s_{45})\,,$$
$$\mathcal{N}^{(7)}_{\text{PBmmz}} = \epsilon^4\, N^{(7)}_{\text{PBmmz}}(X)\Big[(k_1 - p_5)^2 + R^{(7,a)}_{\text{PBmmz}}(X)\,\mu_{12}$$
$$+ R^{(7,b)}_{\text{PBmmz}}(X) \Big] + (\text{sub-sectors})\,, \tag{A.7}$$

where $N^{(7)}_{\text{PBmmz}}(X)$, $R^{(7,a)}_{\text{PBmmz}}(X)$ and $R^{(7,b)}_{\text{PBmmz}}(X)$ are rational functions of X. To construct the fourth numerator, we started from $\epsilon^4\,(k_1 - p_5)^2$, which leads to DEs linear in ϵ, and added terms to achieve the factorisation of ϵ as described in section 3.1.

PBmmz, $\{1,1,1,0,1,1,1,1,0,0,0\}$, 3 MIs
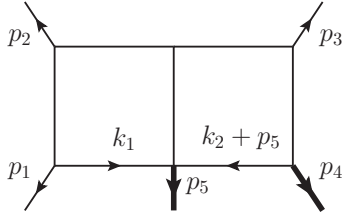
$$\mathcal{N}^{(13)}_{\text{PBmmz}} = \epsilon^4 \sqrt{\Delta_5}\,\mu_{12}\,,$$
$$\mathcal{N}^{(14)}_{\text{PBmmz}} = \epsilon^4\, s_{12}\left[s_{34}\,(k_1 - p_4 - p_5)^2 - s_4\,(k_1 + p_1 + p_2)^2 \right]\,,$$
$$\mathcal{N}^{(15)}_{\text{PBmmz}} = \epsilon^4\, s_{12}s_{23}s_{34}\,. \tag{A.8}$$

PBmzm, $\{1, 1, 1, 1, 1, 1, 0, 1, 0, 0, 0\}$**, 3 MIs**
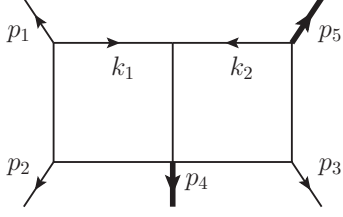
$$\mathcal{N}_{\mathrm{PBmzm}}^{(4)} = \epsilon^4 \sqrt{\Delta_5}\, \mu_{12}\,,$$

$$\mathcal{N}_{\mathrm{PBmzm}}^{(5)} = \epsilon^4\, s_{12}(s_{34} + s_{45} - s_4 - s_{12})\,(k_2 - p_1)^2\,,$$

$$\mathcal{N}_{\mathrm{PBmzm}}^{(6)} = \epsilon^4\, s_{12}(s_4 s_5 - s_4 s_{15} - s_{12} s_{15} - s_5 s_{23}$$

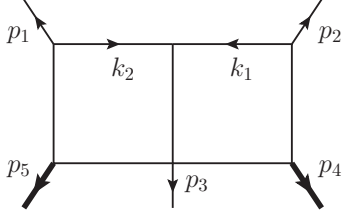$$- s_5 s_{34} + s_{15} s_{34} + s_{15} s_{45})\,. \tag{A.9}$$

PBmzz, $\{1, 1, 1, 0, 1, 1, 1, 1, 0, 0, 0\}$**, 3 MIs**
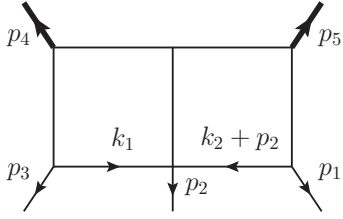
$$\mathcal{N}_{\mathrm{PBmzz}}^{(12)} = \epsilon^4 \sqrt{\Delta_5}\, \mu_{12}\,,$$

$$\mathcal{N}_{\mathrm{PBmzz}}^{(13)} = \epsilon^4\, (s_{12} s_4 s_{15} + s_5 s_{23} s_{34} - s_{15} s_{34} s_{45})\,,$$

$$\mathcal{N}_{\mathrm{PBmzz}}^{(14)} = \epsilon^4\, N_{\mathrm{PBmzz}}^{(14)}(X) \Big[(k_1 - p_2)^2 + R_{\mathrm{PBmzz}}^{(14,a)}(X)\, \mu_{12} \tag{A.10}$$

$$+ R_{\mathrm{PBmzz}}^{(14,b)}(X) \Big] + (\text{sub-sectors})\,,$$

where $N_{\mathrm{PBmzz}}^{(14)}(X)$, $R_{\mathrm{PBmzz}}^{(14,a)}(X)$ and $R_{\mathrm{PBmzz}}^{(14,b)}(X)$ are rational functions of X.

PBzmz, $\{1, 1, 1, 1, 1, 1, 0, 1, 0, 0, 0\}$**, 3 MIs**

$$\mathcal{N}_{\mathrm{PBzmz}}^{(4)} = \epsilon^4 \sqrt{\Delta_5}\, \mu_{12}\,,$$

$$\mathcal{N}_{\mathrm{PBzmz}}^{(5)} = \epsilon^4\, (s_{23} + s_{34} - s_{15}) \left[s_{15}\,(k_1 + p_1)^2 + (s_5 - 2 s_{15})\, k_1^2 \right]\,,$$

$$\mathcal{N}_{\mathrm{PBzmz}}^{(6)} = \epsilon^4\, s_{12} s_{15}(s_{23} + s_{34} - s_4 - s_{15})\,. \tag{A.11}$$

PBzmz, $\{1, 1, 1, 0, 1, 1, 1, 1, 0, 0, 0\}$**, 3 MIs**
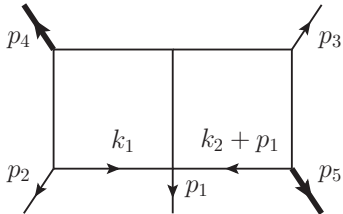
$$\mathcal{N}_{\mathrm{PBzmz}}^{(11)} = \epsilon^4 \sqrt{\Delta_5}\, \mu_{12}\,,$$

$$\mathcal{N}_{\mathrm{PBzmz}}^{(12)} = \epsilon^4\, (s_{15} - s_{23} - s_{34}) \big[s_5\,(k_1 + p_2 + p_4)^2$$

$$- (s_4 + s_5 + s_{12} - s_{34} - s_{45})(k_1 - p_1 - p_5)^2 \big]\,,$$

$$\mathcal{N}_{\mathrm{PBzmz}}^{(13)} = \epsilon^4\, (s_4 s_{15} - s_4 s_{34} - s_{15} s_{34} + s_{23} s_{34} + s_{34}^2)$$

$$\times (s_4 + s_5 + s_{12} - s_{34} - s_{45})\,. \tag{A.12}$$

PBmmz, $\{1,1,1,0,1,1,0,1,0,0,0\}$, 6 MIs
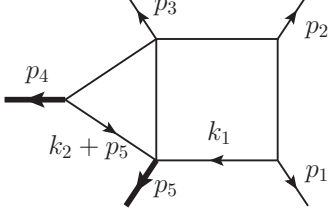
$$\mathcal{N}^{(18)}_{\text{PBmmz}} = \epsilon^3 \sqrt{\Delta_5} \frac{\mu_{12}}{(k_1 + k_2)^2} \,,$$

$$\mathcal{N}^{(19)}_{\text{PBmmz}} = \epsilon^3 \sqrt{\Delta_5} \frac{\mu_{11}}{(k_1 + k_2)^2} \,,$$

$$\mathcal{N}^{(20)}_{\text{PBmmz}} = \epsilon^4 \, s_{12} \sqrt{\lambda(s_{23}, s_4, s_{15})} \,,$$

$$\mathcal{N}^{(21)}_{\text{PBmmz}} = \epsilon^4 \, s_{12} \left[\frac{s_{15} s_4}{\epsilon \, (k_2 + p_5)^2} - (s_4 + s_{15} - s_{23}) \right] \,,$$

$$\mathcal{N}^{(22)}_{\text{PBmmz}} = \epsilon^4 \, s_{12} \left[\frac{s_{23} s_4}{\epsilon \, (k_2 + p_4 + p_5)^2} - (s_4 - s_{15} + s_{23}) \right] \,,$$

$$\mathcal{N}^{(23)}_{\text{PBmmz}} = \epsilon^4 \, s_{12} \left[\frac{s_4 (k_1 - p_5)^2}{\epsilon \, (k_2 + p_5)} - (s_4 + s_{15} - s_{23}) \right] \,.$$

$$\text{(A.13)}$$

PBmmz, $\{1,1,0,0,1,1,1,1,0,0,0\}$, 2 MIs
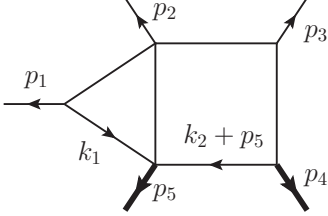
$$\mathcal{N}^{(25)}_{\text{PBmmz}} = \epsilon^3 \sqrt{\Delta_5} \frac{\mu_{22}}{(k_1 + k_2)^2} \,,$$

$$\mathcal{N}^{(26)}_{\text{PBmmz}} = \epsilon^4 \, (s_{12} s_4 + s_{23} s_{34} - s_{34} s_{45}) \,.$$

$$\text{(A.14)}$$

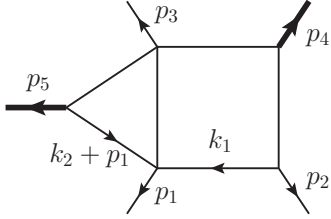**PBmmz, 30, $\{0,1,1,1,1,1,0,1,0,0,0\}$, 2 MIs**

$$\mathcal{N}^{(30)}_{\text{PBmmz}} = \epsilon^3 \sqrt{\Delta_5} \frac{\mu_{22}}{(k_1 + k_2)^2} \,,$$

$$\mathcal{N}^{(31)}_{\text{PBmmz}} = \epsilon^4 \sqrt{r_2^{(1)}} \,,$$
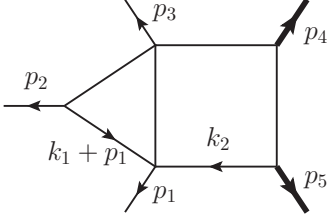
$$\text{(A.15)}$$

where $r_2^{(1)}$ is defined in eq. (3.17).

PBmzm, $\{1,1,1,0,1,1,0,1,0,0,0\}$, 2 MIs

$$\mathcal{N}^{(18)}_{\text{PBmzm}} = \epsilon^3 \sqrt{\Delta_5} \frac{\mu_{11}}{(k_1 + k_2)^2} \,,$$
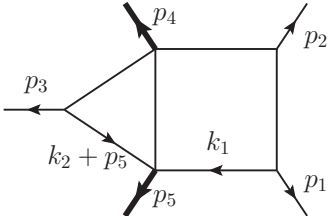
$$\mathcal{N}^{(19)}_{\text{PBmzm}} = \epsilon^4 \, s_{12} (s_{23} + s_{34} - s_4) \,.$$

$$\text{(A.16)}$$

PBmzm, $\{1,1,0,0,1,1,1,1,0,0,0\}$, **2 MIs**

$$\mathcal{N}^{(22)}_{\mathrm{PBmzm}} = \epsilon^3 \sqrt{\Delta_5} \, \frac{\mu_{22}}{(k_1 + k_2)^2} \,,$$
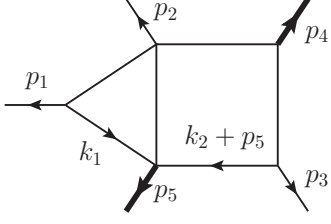
$$\mathcal{N}^{(23)}_{\mathrm{PBmzm}} = \epsilon^4 \left[s_4(s_5 - s_{15}) - s_{34}(s_5 + s_{12} - s_{15} + s_{23} - s_{45}) \right] .$$

$$(\mathrm{A.17})$$

PBmzz, $\{1,1,1,0,1,1,0,1,0,0,0\}$, **2 MIs**

$$\mathcal{N}^{(17)}_{\mathrm{PBmzz}} = \epsilon^3 \sqrt{\Delta_5} \, \frac{\mu_{11}}{(k_1 + k_2)^2} \,,$$
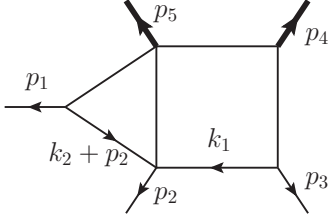
$$\mathcal{N}^{(18)}_{\mathrm{PBmzz}} = \epsilon^4 \left(s_4 s_{12} + s_{23} s_{34} - s_{34} s_{45} \right) .$$

$$(\mathrm{A.18})$$

PBzmz, $\{1,1,1,0,1,1,0,1,0,0,0\}$, **6 MIs**

$$\mathcal{N}^{(16)}_{\mathrm{PBzmz}} = \epsilon^3 \sqrt{\Delta_5} \, \frac{\mu_{12}}{(k_1 + k_2)^2} \,,$$

$$\mathcal{N}^{(17)}_{\mathrm{PBzmz}} = \epsilon^3 \sqrt{\Delta_5} \, \frac{\mu_{11}}{(k_1 + k_2)^2} \,,$$

$$\mathcal{N}^{(18)}_{\mathrm{PBzmz}} = \epsilon^4 \sqrt{r_3^{(3)}} \,,$$

$$\mathcal{N}^{(19)}_{\mathrm{PBzmz}} = \epsilon^4 \left[\frac{s_5 s_{12}(s_{23} + s_{34} - s_4 - s_{15})}{\epsilon \, (k_2 + p_1)^2} \right.$$
$$\left. + s_4(s_{12} + s_{15} - s_{34}) + (s_{12} - s_{34} + s_5)(s_{15} - s_{23} - s_{34}) \right] ,$$

$$\mathcal{N}^{(20)}_{\mathrm{PBzmz}} = \epsilon^4 \left[\frac{s_5 \big(s_4(s_{15} - s_{34}) + s_{34}(s_{23} + s_{34} - s_{15})\big)}{\epsilon \, (k_2 + p_1 + p_5)^2} \right.$$
$$\left. - s_4(s_{12} + s_{15} - s_{34}) - (s_{12} - s_{34} - s_5)(s_{15} - s_{23} - s_{34}) \right] ,$$

$$\mathcal{N}^{(21)}_{\mathrm{PBzmz}} = \epsilon^4 \left[\frac{s_5(s_{23} + s_{34} - s_{15})\,(k_1 - p_1)^2}{\epsilon \, (k_2 + p_1)^2} \right.$$
$$\left. + s_4(s_{12} + s_{15} - s_{34}) + (s_{12} - s_{34} + s_5)(s_{15} - s_{23} - s_{34}) \right] ,$$
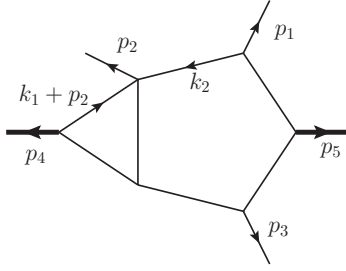
$$(\mathrm{A.19})$$

where $r_3^{(3)}$ is obtained by swapping $p_4 \leftrightarrow p_5$ and $p_1 \leftrightarrow p_2$ in $r_3^{(1)}$, defined in eq. (3.18).

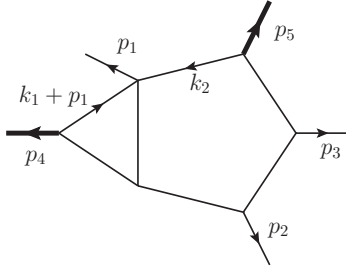**PBmzz, $\{0, 1, 1, 1, 1, 1, 1, 1, 0, 0, 0\}$, 1 MI**
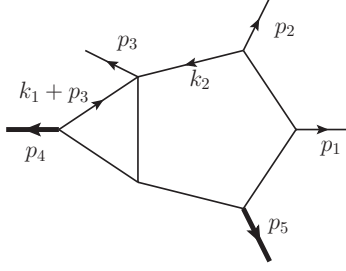
$$\mathcal{N}_{\text{PBmzz}}^{(15)} = \epsilon^4 \sqrt{\Delta_5} \, \mu_{22} \, . \qquad \text{(A.20)}$$

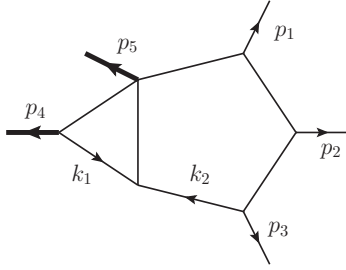**PBzmz, $\{0, 1, 1, 1, 1, 1, 1, 1, 0, 0, 0\}$, 1 MI**

$$\mathcal{N}_{\text{PBzmz}}^{(14)} = \epsilon^4 \sqrt{\Delta_5} \, \mu_{22} \, . \qquad \text{(A.21)}$$

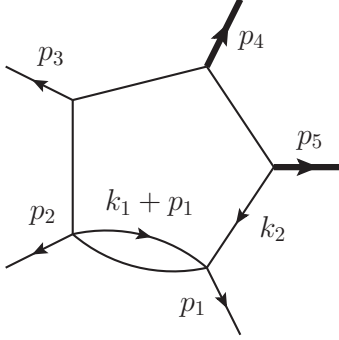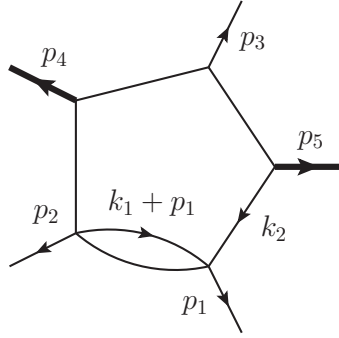**PBzzm, $\{0, 1, 1, 1, 1, 1, 1, 1, 0, 0, 0\}$, 1 MI**

$$\mathcal{N}_{\text{PBzzm}}^{(15)} = \epsilon^4 \sqrt{\Delta_5} \, \mu_{22} \, . \qquad \text{(A.22)}$$

PBzzz, $\{1, 1, 0, 1, 1, 1, 1, 1, 0, 0, 0\}$, 1 MI

$$\mathcal{N}_{\text{PBzzz}}^{(20)} = \epsilon^4 \sqrt{\Delta_5} \, \frac{s_{12}s_{23}(s_4 s_{12} s_{15} + s_5 s_{23} s_{34} - s_{15} s_{34} s_{45})}{\Delta_5}$$
$$+ \, (\text{sub-sectors}) \, . \qquad \text{(A.23)}$$

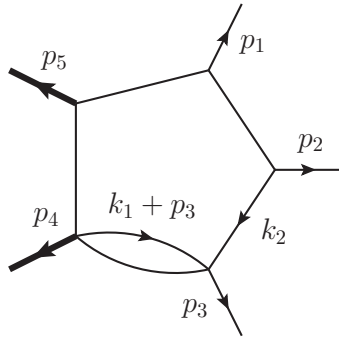**PBmmz,** $\{0, 1, 0, 1, 1, 1, 1, 1, 0, 0, 0\}$**, 2 MIs**

$$\mathcal{N}^{(32)}_{\text{PBmmz}} = \epsilon^3 \sqrt{\Delta_5} \frac{\mu_{22}}{(k_1 + k_2)^2} \,,$$

$$\mathcal{N}^{(33)}_{\text{PBmmz}} = \epsilon^3 (1 - 2\epsilon)(s_{34}s_{45} - s_4 s_{12}) \,. \tag{A.24}$$

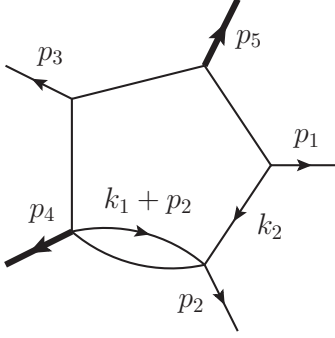**PBmzm,** $\{0, 1, 0, 1, 1, 1, 1, 1, 0, 0, 0\}$**, 2 MIs**

$$\mathcal{N}^{(29)}_{\text{PBmzm}} = \epsilon^3 \sqrt{\Delta_5} \frac{\mu_{22}}{(k_1 + k_2)^2} \,,$$

$$\mathcal{N}^{(30)}_{\text{PBmzm}} = \epsilon^3 (1 - 2\epsilon)(s_4 s_5 - s_4 s_{34} - s_5 s_{34} - s_{12} s_{34}$$
$$+ s_{34}^2 + s_{34} s_{45}) \,. \tag{A.25}$$

PBmzz, $\{0, 1, 0, 1, 1, 1, 1, 1, 0, 0, 0\}$**, 2 MIs**

$$\mathcal{N}^{(36)}_{\text{PBmzz}} = \epsilon^3 \sqrt{\Delta_5} \frac{\mu_{22}}{(k_1 + k_2)^2} \,,$$

$$\mathcal{N}^{(37)}_{\text{PBmzz}} = \epsilon^3 (1 - 2\epsilon) \, s_{12} \, s_{15} \,. \tag{A.26}$$
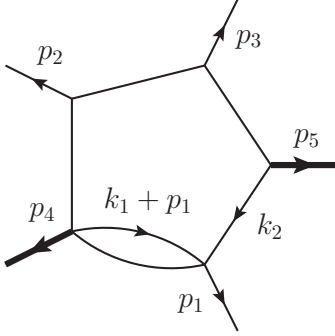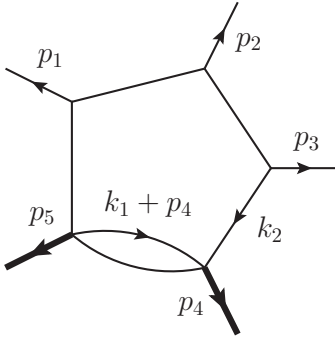
PBzmz, $\{0, 1, 0, 1, 1, 1, 1, 1, 0, 0, 0\}$, **2 MIs**

$$\mathcal{N}_{\text{PBzmz}}^{(38)} = \epsilon^3 \sqrt{\Delta_5} \frac{\mu_{22}}{(k_1 + k_2)^2} \,,$$

$$\mathcal{N}_{\text{PBzmz}}^{(39)} = \epsilon^3 (1 - 2\epsilon)(s_4 s_{15} - s_4 s_5 + s_{12} s_{15}$$
$$+ s_5 s_{23} + s_5 s_{34} - s_{15} s_{34} - s_{15} s_{45}) \,. \tag{A.27}$$

PBzzm, $\{0, 1, 0, 1, 1, 1, 1, 1, 0, 0, 0\}$, **2 MIs**

$$\mathcal{N}_{\text{PBzzm}}^{(36)} = \epsilon^3 \sqrt{\Delta_5} \frac{\mu_{22}}{(k_1 + k_2)^2} \,,$$

$$\mathcal{N}_{\text{PBzzm}}^{(37)} = \epsilon^3 (1 - 2\epsilon)\, s_{23}(s_4 + s_5 + s_{12} - s_{34} - s_{45}) \,. \tag{A.28}$$

PBzzz, $\{0, 1, 0, 1, 1, 1, 1, 1, 0, 0, 0\}$, **2 MIs**

$$\mathcal{N}_{\text{PBzzz}}^{(49)} = \epsilon^3 \sqrt{\Delta_5} \frac{\mu_{22}}{(k_1 + k_2)^2} \,,$$

$$\mathcal{N}_{\text{PBzzz}}^{(50)} = \epsilon^3 (1 - 2\epsilon)\, s_{12}\, s_{23} \,. \tag{A.29}$$

B Kinematic Regions

In section 3.3 we introduced two regions of phase space where we obtained numerical evaluations of our integrals, namely the Euclidean region and the s_{12}-channel. In section section 4.3 we further introduced the amplituhedron region $\mathbb{A}$. In this appendix we define these regions explicitly.

Let us first discuss the Euclidean region. Given the non-cyclic indexing of the external legs in the integral families in figs. 1 and 2, the Euclidean region associated with each one of those families

is not necessarily the same. We define our Euclidean region as the intersection of the Euclidean regions associated with any permutation of the representative families given in figs. 1 and 2, i.e.,

$$s_{ij} < 0, \qquad s_4 < 0, \qquad s_5 < 0, \tag{B.1}$$

for $i \neq j = 1, \ldots, 5$. Note that this region is not guaranteed to be non-empty, but it is in our case and the point in eq. (3.20) lies within it.

The second kinematic region we consider is what we call the 's_{12}-channel', corresponding to the process where legs p_1 and p_2 are in the initial state, and legs p_3, p_4 and p_5 are in the final state, that is $-p_1 - p_2 \rightarrow p_3 + p_4 + p_5$. For instance, such a process could describe the production of two vector bosons in association with a jet at an hadron collider, and as such is of phenomenological interest. This channel is defined by the following set of constraints:

$$p_1 \cdot p_2 > 0, \quad p_3 \cdot p_4 > 0, \quad p_4 \cdot p_5 > 0, \quad p_3 \cdot p_5 > 0,$$
$$p_1 \cdot p_3 < 0, \quad p_1 \cdot p_4 < 0, \quad p_1 \cdot p_5 < 0, \quad p_2 \cdot p_3 < 0, \quad p_2 \cdot p_4 < 0, \quad p_2 \cdot p_5 < 0,$$
$$G(p_4) = 2\, s_4 > 0, \quad G(p_5) = 2\, s_5 > 0, \tag{B.2}$$
$$G(p_i, p_j) < 0, \quad G(p_i, p_j, p_k) > 0, \quad G(p_1, p_2, p_3, p_4) < 0,$$

where i, j and k take distinct values in $\{1, 2, 3, 4, 5\}$. The point X_1 in eq. (3.22) lies within the kinematic region defined by these constraints, and is furthermore 'generic', in the sense that none of the letters of the alphabet for integrals for five-point two-loop integrals with two external masses vanish or diverge there. Having in mind the construction of pentagon functions for this set of integrals, we choose another point within the s_{12}-channel that also has the symmetries of the region. In this case, this means that it is invariant under the exchanges $1 \leftrightarrow 2$ and $4 \leftrightarrow 5$. The point X_0 in eq. (3.21) satisfies these conditions.

Finally, let us explain the origin of the inequalities in eqs. (4.30) and (4.31) which specify the amplituhedron region. We represent the Lagrangian coordinates x_0, $x_{0'}$ by bi-twistors $Z_A Z_B$ and $Z_C Z_D$, and choose $x_{0'} \rightarrow \infty$ by taking $Z_C Z_D$ to be the infinity bi-twistor. The momentum twistors $Z_1, \ldots, Z_4$ represent the quadrilateral light-like contour. The two-loop four-particle MHV amplituhedron is specified by the following inequalities for the four-brackets of momentum twistors [102],

$$\langle AB12 \rangle, \langle AB23 \rangle, \langle AB34 \rangle, \langle AB14 \rangle, \langle CD12 \rangle, \langle CD23 \rangle, \langle CD34 \rangle, \langle CD14 \rangle, \langle ABCD \rangle > 0, \tag{B.3}$$

$$\langle CD13 \rangle, \langle CD24 \rangle < 0, \tag{B.4}$$

$$\langle AB13 \rangle, \langle AB24 \rangle < 0. \tag{B.5}$$

The inequalities (B.3) and (B.4) are equivalent to those in eq. (4.30) when written in dual momenta variables, and as such they impose the condition of being in the anti-Euclidean region. As already noted below eq. (4.12), working in the anti-Euclidean region instead of the Euclidean region is purely conventional, and the same non-trivial positivity conclusions hold in the Euclidean region. The inequalities (B.5) imply that

$$x_{13}^2(x_{20}^2 + x_{40}^2) + x_{24}^2(x_{10}^2 + x_{30}^2) - x_{13}^2 x_{24}^2 \pm \epsilon_5 > 0 \tag{B.6}$$

where the pseudo-scalar invariant $\epsilon_5 := \mathrm{tr}(\slashed{p}_{12}\slashed{p}_{23}\slashed{p}_{34}\slashed{p}_{10}\gamma_5)$ is related to the $\bar{\Delta}_5$ defined in eq. (4.24) through $(\epsilon_5)^2 = \bar{\Delta}_5$. Thus, the space-time coordinates are complex valued in such a way that the Mandelstam invariants and ϵ_5 are real-valued. The constraints in eq. (4.31) then follow.

References

[1] J.L. Bourjaily et al., *Functions Beyond Multiple Polylogarithms for Precision Collider Physics*, in *Snowmass 2021*, 3, 2022 [2203.07088]. (cited on page 1)

[2] K.-T. Chen, *Iterated path integrals*, *Bull. Am. Math. Soc.* **83** (1977) 831. (cited on pages 1, 7, and 12)

[3] N. Arkani-Hamed, J.L. Bourjaily, F. Cachazo and J. Trnka, *Local Integrals for Planar Scattering Amplitudes*, *JHEP* **06** (2012) 125 [1012.6032]. (cited on pages 1, 6, 7, and 20)

[4] J.M. Henn, *Multiloop integrals in dimensional regularization made simple*, *Phys. Rev. Lett.* **110** (2013) 251601 [1304.1806]. (cited on pages 1, 2, and 6)

[5] S. Abreu, R. Britto and C. Duhr, *The SAGEX review on scattering amplitudes Chapter 3: Mathematical structures in Feynman integrals*, *J. Phys. A* **55** (2022) 443004 [2203.13014]. (cited on pages 1 and 13)

[6] S. Abreu, R. Britto, C. Duhr and E. Gardi, *Diagrammatic Hopf algebra of cut Feynman integrals: the one-loop case*, *JHEP* **12** (2017) 090 [1704.07931]. (cited on page 2)

[7] N. Arkani-Hamed and E.Y. Yuan, *One-Loop Integrals from Spherical Projections of Planes and Quadrics*, 1712.09991. (cited on page 2)

[8] J. Chen, B. Feng and L.L. Yang, *Intersection theory rules symbology*, *Sci. China Phys. Mech. Astron.* **67** (2024) 221011 [2305.01283]. (cited on page 2)

[9] C. Fevola, S. Mizera and S. Telen, *Landau Singularities Revisited: Computational Algebraic Geometry for Feynman Integrals*, *Phys. Rev. Lett.* **132** (2024) 101601 [2311.14669]. (cited on pages 2, 9, and 11)

[10] C. Fevola, S. Mizera and S. Telen, *Principal Landau Determinants*, *Comput. Phys. Commun.* **303** (2024) 109278 [2311.16219]. (cited on pages 2 and 9)

[11] X. Jiang and L.L. Yang, *The recursive structure of Baikov representations I: Generics and application to symbology*, *Phys. Rev. D* **108** (2023) 076004 [2303.11657]. (cited on pages 2 and 9)

[12] C. Dlapa, M. Helmer, G. Papathanasiou and F. Tellander, *Symbol alphabets from the Landau singular locus*, *JHEP* **10** (2023) 161 [2304.02629]. (cited on pages 2 and 9)

[13] S. He, X. Jiang, J. Liu and Q. Yang, *On symbology and differential equations of Feynman integrals from Schubert analysis*, *JHEP* **12** (2023) 140 [2309.16441]. (cited on pages 2 and 9)

[14] X. Jiang, J. Liu, X. Xu and L.L. Yang, *Symbol letters of Feynman integrals from Gram determinants*, 2401.07632. (cited on pages 2, 6, 8, 9, and 26)

[15] M. Helmer, G. Papathanasiou and F. Tellander, *Landau Singularities from Whitney Stratifications*, 2402.14787. (cited on page 2)

[16] S. Caron-Huot, M. Correia and M. Giroux, *Recursive Landau Analysis*, 2406.05241. (cited on pages 2, 9, and 11)

[17] H.S. Hannesdottir, A.J. McLeod, M.D. Schwartz and C. Vergu, *Implications of the Landau equations for iterated integrals*, *Phys. Rev. D* **105** (2022) L061701 [2109.09744]. (cited on page 2)

[18] H.S. Hannesdottir, L. Lippstreu, A.J. McLeod and M. Polackova, *Minimal Cuts and Genealogical Constraints on Feynman Integrals*, 2406.05943. (cited on page 2)

[19] R.N. Lee, *Reducing differential equations for multiloop master integrals*, *JHEP* **04** (2015) 108 [1411.0911]. (cited on page 2)

[20] C. Meyer, *Algorithmic transformation of multi-loop master integrals to a canonical basis with CANONICA*, *Comput. Phys. Commun.* **222** (2018) 295 [1705.06252]. (cited on page 2)

[21] M. Prausa, *epsilon: A tool to find a canonical basis of master integrals*, *Comput. Phys. Commun.* **219** (2017) 361 [1701.00725]. (cited on page 2)

[22] O. Gituliar and V. Magerya, *Fuchsia: a tool for reducing differential equations for Feynman master integrals to epsilon form*, *Comput. Phys. Commun.* **219** (2017) 329 [1701.04269]. (cited on page 2)

[23] R.N. Lee, *Libra: A package for transformation of differential systems for multiloop integrals*, *Comput. Phys. Commun.* **267** (2021) 108058 [2012.00279]. (cited on page 2)

[24] J. Henn, B. Mistlberger, V.A. Smirnov and P. Wasser, *Constructing d-log integrands and computing master integrals for three-loop four-particle scattering*, *JHEP* **04** (2020) 167 [`2002.09492`]. (cited on pages 2 and 21)

[25] J. Chen, X. Jiang, X. Xu and L.L. Yang, *Constructing canonical Feynman integrals with intersection theory*, *arXiv [hep-th]* **814** (2021) 136085 [`2008.03045`]. (cited on page 2)

[26] J. Chen, X. Jiang, C. Ma, X. Xu and L.L. Yang, *Baikov representations, intersection theory, and canonical Feynman integrals*, *arXiv [hep-th]* **07** (2022) 066 [`2202.08127`]. (cited on page 2)

[27] C. Dlapa, J. Henn and K. Yan, *Deriving canonical differential equations for Feynman integrals from a single uniform weight integral*, *JHEP* **05** (2020) 025 [`2002.02340`]. (cited on page 2)

[28] C. Dlapa, X. Li and Y. Zhang, *Leading singularities in Baikov representation and Feynman integrals with uniform transcendental weight*, *JHEP* **07** (2021) 227 [`2103.04638`]. (cited on pages 2, 8, and 10)

[29] S. Abreu, H. Ita, F. Moriello, B. Page, W. Tschernow and M. Zeng, *Two-Loop Integrals for Planar Five-Point One-Mass Processes*, *JHEP* **11** (2020) 117 [`2005.04195`]. (cited on pages 2, 6, and 8)

[30] S. Abreu, H. Ita, B. Page and W. Tschernow, *Two-loop hexa-box integrals for non-planar five-point one-mass processes*, *JHEP* **03** (2022) 182 [`2107.14180`]. (cited on pages 2 and 9)

[31] S. Abreu, D. Chicherin, H. Ita, B. Page, V. Sotnikov, W. Tschernow et al., *All Two-Loop Feynman Integrals for Five-Point One-Mass Scattering*, *Phys. Rev. Lett.* **132** (2024) 141601 [`2306.15431`]. (cited on pages 2, 11, 13, and 24)

[32] J.M. Henn, A. Matijašić, J. Miczajka, T. Peraro, Y. Xu and Y. Zhang, *A computation of two-loop six-point Feynman integrals in dimensional regularization*, `2403.19742`. (cited on page 2)

[33] F. Febres Cordero, G. Figueiredo, M. Kraus, B. Page and L. Reina, *Two-loop master integrals for leading-color $pp \to t\bar{t}H$ amplitudes with a light-quark loop*, *JHEP* **07** (2024) 084 [`2312.08131`]. (cited on page 2)

[34] S. Badger, M. Becchetti, E. Chaubey and R. Marzucca, *Two-loop master integrals for a planar topology contributing to $pp \to t\bar{t}j$*, *JHEP* **01** (2023) 156 [`2210.17477`]. (cited on pages 2 and 8)

[35] S. Badger, M. Becchetti, N. Giraudo and S. Zoia, *Two-loop integrals for $t\bar{t}$+jet production at hadron colliders in the leading colour approximation*, *JHEP* **07** (2024) 073 [`2404.12325`]. (cited on pages 2 and 8)

[36] D. Chicherin and V. Sotnikov, *Pentagon Functions for Scattering of Five Massless Particles*, *JHEP* **20** (2020) 167 [`2009.07803`]. (cited on pages 2 and 13)

[37] D. Chicherin, V. Sotnikov and S. Zoia, *Pentagon functions for one-mass planar scattering amplitudes*, *JHEP* **01** (2022) 096 [`2110.10111`]. (cited on pages 2, 12, and 13)

[38] A. von Manteuffel and R.M. Schabinger, *A novel approach to integration by parts reduction*, *Phys. Lett. B* **744** (2015) 101 [`1406.4513`]. (cited on pages 2 and 6)

[39] T. Peraro, *Scattering amplitudes over finite fields and multivariate functional reconstruction*, *JHEP* **12** (2016) 030 [`1608.01902`]. (cited on pages 2 and 6)

[40] T. Peraro, *FiniteFlow: multivariate functional reconstruction using finite fields and dataflow graphs*, *JHEP* **07** (2019) 031 [`1905.08019`]. (cited on pages 2, 5, and 6)

[41] L.F. Alday and J.M. Maldacena, *Gluon scattering amplitudes at strong coupling*, *JHEP* **06** (2007) 064 [`0705.0303`]. (cited on pages 2 and 14)

[42] J.M. Drummond, G.P. Korchemsky and E. Sokatchev, *Conformal properties of four-gluon planar amplitudes and Wilson loops*, *Nucl. Phys. B* **795** (2008) 385 [`0707.0243`]. (cited on pages 2 and 14)

[43] A. Brandhuber, P. Heslop and G. Travaglini, *MHV amplitudes in N=4 super Yang-Mills and Wilson loops*, *Nucl. Phys. B* **794** (2008) 231 [`0707.1153`]. (cited on page 2)

[44] N. Arkani-Hamed, J.L. Bourjaily, F. Cachazo, A.B. Goncharov, A. Postnikov and J. Trnka, *Grassmannian Geometry of Scattering Amplitudes*, Cambridge University Press (4, 2016), 10.1017/CBO9781316091548, [1212.5605]. (cited on pages 2 and 21)

[45] L.F. Alday, E.I. Buchbinder and A.A. Tseytlin, *Correlation function of null polygonal Wilson loops with local operators*, *JHEP* **09** (2011) 034 [1107.5702]. (cited on pages 2 and 16)

[46] L.F. Alday, P. Heslop and J. Sikorowski, *Perturbative correlation functions of null Wilson loops and local operators*, *JHEP* **03** (2013) 074 [1207.4316]. (cited on pages 2 and 16)

[47] L.F. Alday, J.M. Henn and J. Sikorowski, *Higher loop mixed correlators in N=4 SYM*, *JHEP* **03** (2013) 058 [1301.0149]. (cited on pages 2 and 16)

[48] J.M. Henn, G.P. Korchemsky and B. Mistlberger, *The full four-loop cusp anomalous dimension in $\mathcal{N} = 4$ super Yang-Mills and QCD*, *JHEP* **04** (2020) 018 [1911.10174]. (cited on pages 2 and 16)

[49] D. Chicherin and J.M. Henn, *Symmetry properties of Wilson loops with a Lagrangian insertion*, *JHEP* **07** (2022) 057 [2202.05596]. (cited on pages 2, 3, 17, and 24)

[50] D. Chicherin and J. Henn, *Pentagon Wilson loop with Lagrangian insertion at two loops in $\mathcal{N} = 4$ super Yang-Mills theory*, *JHEP* **07** (2022) 038 [2204.00329]. (cited on pages 2, 18, and 23)

[51] N. Arkani-Hamed and J. Trnka, *The Amplituhedron*, *JHEP* **10** (2014) 030 [1312.2007]. (cited on pages 2 and 22)

[52] N. Arkani-Hamed, J. Henn and J. Trnka, *Nonperturbative negative geometries: amplitudes at strong coupling and the amplituhedron*, *JHEP* **03** (2022) 108 [2112.06956]. (cited on pages 3, 16, 17, and 23)

[53] T.V. Brown, U. Oktem, S. Paranjape and J. Trnka, *Loops of loops expansion in the amplituhedron*, *JHEP* **07** (2024) 025 [2312.17736]. (cited on pages 3 and 16)

[54] J.M. Henn, M. Lagares and S.-Q. Zhang, *Integrated negative geometries in ABJM*, *JHEP* **05** (2023) 112 [2303.02996]. (cited on page 3)

[55] S. He, C.-K. Kuo, Z. Li and Y.-Q. Zhang, *Emergent unitarity, all-loop cuts and integrations from the ABJM amplituhedron*, *JHEP* **07** (2023) 212 [2303.03035]. (cited on page 3)

[56] M. Lagares and S.-Q. Zhang, *Higher-loop integrated negative geometries in ABJM*, *JHEP* **05** (2024) 142 [2402.17432]. (cited on page 3)

[57] J. Henn and P. Raman, *Positivity properties of scattering amplitudes*, 2407.05755. (cited on page 3)

[58] S. Abreu, D. Chicherin, V. Sotnikov and S. Zoia, *Ancillary files for "Two-Loop Five-Point Two-Mass Planar Integrals and Double Lagrangian Insertions in a Wilson Loop"*, 8, 2024. 10.5281/zenodo.13254698. (cited on pages 3, 5, 9, and 24)

[59] F.V. Tkachov, *A Theorem on Analytical Calculability of Four Loop Renormalization Group Functions*, *Phys. Lett.* **100B** (1981) 65. (cited on page 5)

[60] K.G. Chetyrkin and F.V. Tkachov, *Integration by Parts: The Algorithm to Calculate beta Functions in 4 Loops*, *Nucl. Phys. B* **192** (1981) 159. (cited on page 5)

[61] R.N. Lee, *Presenting LiteRed: a tool for the Loop InTEgrals REDuction*, 1212.2685. (cited on pages 5 and 6)

[62] R.N. Lee, *LiteRed 1.4: a powerful tool for reduction of multiloop integrals*, *J. Phys. Conf. Ser.* **523** (2014) 012059 [1310.1145]. (cited on pages 5 and 6)

[63] Z. Wu, J. Boehm, R. Ma, H. Xu and Y. Zhang, *NeatIBP 1.0, a package generating small-size integration-by-parts relations for Feynman integrals*, *Comput. Phys. Commun.* **295** (2024) 108999 [2305.08783]. (cited on pages 5 and 6)

[64] S. Laporta, *High precision calculation of multiloop Feynman integrals by difference equations*, *Int. J. Mod. Phys.* **A15** (2000) 5087 [hep-ph/0102033]. (cited on pages 5 and 6)

[65] T. Peraro, *Analytic multi-loop results using finite fields and dataflow graphs with FiniteFlow*, in *14th International Symposium on Radiative Corrections: Application of Quantum Field Theory to Phenomenology*, 12, 2019, DOI [1912.03142]. (cited on pages 5 and 6)

[66] J. Gluza, K. Kajda and D.A. Kosower, *Towards a Basis for Planar Two-Loop Integrals*, *Phys. Rev. D* **83** (2011) 045012 [1009.0472]. (cited on page 6)

[67] S. Abreu, J. Dormans, F. Febres Cordero, H. Ita and B. Page, *Analytic Form of Planar Two-Loop Five-Gluon Scattering Amplitudes in QCD*, *Phys. Rev. Lett.* **122** (2019) 082002 [1812.04586]. (cited on page 7)

[68] S. Badger, C. Brønnum-Hansen, D. Chicherin, T. Gehrmann, H.B. Hartanto, J. Henn et al., *Virtual QCD corrections to gluon-initiated diphoton plus jet production at hadron colliders*, *JHEP* **11** (2021) 083 [2106.08664]. (cited on page 7)

[69] A.B. Goncharov, M. Spradlin, C. Vergu and A. Volovich, *Classical Polylogarithms for Amplitudes and Wilson Loops*, *Phys. Rev. Lett.* **105** (2010) 151605 [1006.5703]. (cited on pages 7 and 13)

[70] S. Abreu, B. Page and M. Zeng, *Differential equations from unitarity cuts: nonplanar hexa-box integrals*, *JHEP* **01** (2019) 006 [1807.11522]. (cited on page 9)

[71] M. Heller, A. von Manteuffel and R.M. Schabinger, *Multiple polylogarithms with algebraic arguments and the two-loop EW-QCD Drell-Yan master integrals*, *Phys. Rev. D* **102** (2020) 016025 [1907.00491]. (cited on page 9)

[72] S. Zoia, *Modern Analytic Methods for Computing Scattering Amplitudes: With Application to Two-Loop Five-Particle Processes*, Springer International Publishing (2022), 10.1007/978-3-031-01945-6. (cited on page 9)

[73] X. Liu, Y.-Q. Ma and C.-Y. Wang, *A Systematic and Efficient Method to Compute Multi-loop Master Integrals*, *Phys. Lett. B* **779** (2018) 353 [1711.09572]. (cited on pages 11 and 21)

[74] X. Liu and Y.-Q. Ma, *AMFlow: A Mathematica package for Feynman integrals computation via auxiliary mass flow*, *Comput. Phys. Commun.* **283** (2023) 108565 [2201.11669]. (cited on pages 11 and 21)

[75] M. Hidding, *DiffExp, a Mathematica package for computing Feynman integrals in terms of one-dimensional series expansions*, *Comput. Phys. Commun.* **269** (2021) 108125 [2006.05510]. (cited on pages 12 and 21)

[76] D. Gaiotto, J. Maldacena, A. Sever and P. Vieira, *Pulling the straps of polygons*, *JHEP* **12** (2011) 011 [1102.0062]. (cited on page 12)

[77] T. Gehrmann, J.M. Henn and N.A. Lo Presti, *Pentagon functions for massless planar scattering amplitudes*, *JHEP* **10** (2018) 103 [1807.09812]. (cited on page 13)

[78] S. Badger, H.B. Hartanto and S. Zoia, *Two-Loop QCD Corrections to $W b\bar{b}$ Production at Hadron Colliders*, *Phys. Rev. Lett.* **127** (2021) 012001 [2102.02516]. (cited on pages 13 and 21)

[79] S. Badger, J. Kryś, R. Moodie and S. Zoia, *Lepton-pair scattering with an off-shell and an on-shell photon at two loops in massless QED*, *JHEP* **11** (2023) 041 [2307.03098]. (cited on page 13)

[80] I.A. Korchemskaya and G.P. Korchemsky, *On lightlike Wilson loops*, *Phys. Lett. B* **287** (1992) 169. (cited on page 14)

[81] A. Bassetto, I.A. Korchemskaya, G.P. Korchemsky and G. Nardelli, *Gauge invariance and anomalous dimensions of a light cone Wilson loop in lightlike axial gauge*, *Nucl. Phys. B* **408** (1993) 62 [hep-ph/9303314]. (cited on page 14)

[82] G.P. Korchemsky and G. Marchesini, *Structure function for large x and renormalization of Wilson loop*, *Nucl. Phys. B* **406** (1993) 225 [hep-ph/9210281]. (cited on page 14)

[83] G.P. Korchemsky and A.V. Radyushkin, *Loop Space Formalism and Renormalization Group for the Infrared Asymptotics of QCD*, *Phys. Lett. B* **171** (1986) 459. (cited on page 14)

[84] G.P. Korchemsky and A.V. Radyushkin, *Renormalization of the Wilson Loops Beyond the Leading Order*, *Nucl. Phys. B* **283** (1987) 342. (cited on page 14)

[85] B. Eden, G.P. Korchemsky and E. Sokatchev, *From correlation functions to scattering amplitudes*, *JHEP* **12** (2011) 002 [1007.3246]. (cited on page 14)

[86] B. Eden, G.P. Korchemsky and E. Sokatchev, *More on the duality correlators/amplitudes*, *Phys. Lett. B* **709** (2012) 247 [1009.2488]. (cited on page 14)

[87] L.J. Mason and D. Skinner, *The Complete Planar S-matrix of N=4 SYM as a Wilson Loop in Twistor Space*, *JHEP* **12** (2010) 018 [1009.2225]. (cited on page 14)

[88] B. Eden, C. Schubert and E. Sokatchev, *Three loop four point correlator in N=4 SYM*, *Phys. Lett. B* **482** (2000) 309 [hep-th/0003096]. (cited on page 14)

[89] B. Eden, P. Heslop, G.P. Korchemsky and E. Sokatchev, *The super-correlator/super-amplitude duality: Part I*, *Nucl. Phys. B* **869** (2013) 329 [1103.3714]. (cited on page 14)

[90] E. Remiddi and J.A.M. Vermaseren, *Harmonic polylogarithms*, *Int. J. Mod. Phys. A* **15** (2000) 725 [hep-ph/9905237]. (cited on page 16)

[91] Z. Bern, L.J. Dixon and V.A. Smirnov, *Iteration of planar amplitudes in maximally supersymmetric Yang-Mills theory at three loops and beyond*, *Phys. Rev. D* **72** (2005) 085001 [hep-th/0505205]. (cited on page 18)

[92] Z. Bern, M. Czakon, L.J. Dixon, D.A. Kosower and V.A. Smirnov, *The Four-Loop Planar Amplitude and Cusp Anomalous Dimension in Maximally Supersymmetric Yang-Mills Theory*, *Phys. Rev. D* **75** (2007) 085010 [hep-th/0610248]. (cited on page 18)

[93] J.M. Henn, K. Melnikov and V.A. Smirnov, *Two-loop planar master integrals for the production of off-shell vector bosons in hadron collisions*, *JHEP* **05** (2014) 090 [1402.7078]. (cited on pages 19 and 20)

[94] W. Wasow, *Asymptotic expansions for ordinary differential equations*, Pure and Applied Mathematics, Vol. XIV, Interscience Publishers John Wiley & Sons, Inc., New York-London-Sydney (1965). (cited on page 19)

[95] S. Caron-Huot, D. Chicherin, J. Henn, Y. Zhang and S. Zoia, *Multi-Regge Limit of the Two-Loop Five-Point Amplitudes in $\mathcal{N} = 4$ Super Yang-Mills and $\mathcal{N} = 8$ Supergravity*, *JHEP* **10** (2020) 188 [2003.03120]. (cited on page 19)

[96] V.A. Smirnov, *Applied asymptotic expansions in momenta and masses*, Springer Tracts Mod. Phys. **177** (2002) 1. (cited on page 19)

[97] A.V. Kotikov and L.N. Lipatov, *DGLAP and BFKL equations in the $N = 4$ supersymmetric gauge theory*, *Nucl. Phys. B* **661** (2003) 19 [hep-ph/0208220]. (cited on page 20)

[98] D. Chicherin, J.M. Henn and G. Papathanasiou, *Cluster algebras for Feynman integrals*, *Phys. Rev. Lett.* **126** (2021) 091603 [2012.12285]. (cited on page 20)

[99] L. Bossinger, J.M. Drummond and R. Glew, *Adjacency for scattering amplitudes from the Gröbner fan*, *JHEP* **11** (2023) 002 [2212.08931]. (cited on page 20)

[100] Z. Bern, E. Herrmann, S. Litsey, J. Stankowicz and J. Trnka, *Logarithmic Singularities and Maximally Supersymmetric Amplitudes*, *JHEP* **06** (2015) 202 [1412.8584]. (cited on page 21)

[101] F. Moriello, *Generalised power series expansions for the elliptic planar families of Higgs + jet production at two loops*, *JHEP* **01** (2020) 150 [1907.13234]. (cited on page 21)

[102] N. Arkani-Hamed, H. Thomas and J. Trnka, *Unwinding the Amplituhedron in Binary*, *JHEP* **01** (2018) 016 [1704.05069]. (cited on pages 22 and 33)

[103] N. Arkani-Hamed, A. Hodges and J. Trnka, *Positive Amplitudes In The Amplituhedron*, *JHEP* **08** (2015) 030 [1412.8478]. (cited on page 23)

[104] L.J. Dixon, M. von Hippel, A.J. McLeod and J. Trnka, *Multi-loop positivity of the planar $\mathcal{N} = 4$ SYM six-point amplitude*, *JHEP* **02** (2017) 112 [`1611.08325`]. (cited on page 23)